NAVAL POSTGRADUATE SCHOOL

MONTEREY, CALIFORNIA

THESIS

NUMERICAL STUDY FOR OPTIMUM PARAMETERS OF BONDED COMPOSITE REPAIRS OF CRACKED ALUMINUM

by

Aaron S. McGee

June 2012

Thesis Advisor:	Young W. Kwon
Second Reader:	Jarema M. Didoszak

Approved for public release; distribution is unlimited

THIS PAGE INTENTIONALLY LEFT BLANK

REPORT DOCUMENTATION PAGE			Form Approved OMB No. 0704-0188
Public reporting burden for this collection of information is estimated to average 1 hour per response, including the time for reviewing instruction, searching existing data sources, gathering and maintaining the data needed, and completing and reviewing the collection of information. Send comments regarding this burden estimate or any other aspect of this collection of information, including suggestions for reducing this burden, to Washington headquarters Services, Directorate for Information Operations and Reports, 1215 Jefferson Davis Highway, Suite 1204, Arlington, VA 22202-4302, and to the Office of Management and Budget, Paperwork Reduction Project (0704-0188) Washington DC 20503.			
1. AGENCY USE ONLY *(Leave blank)*	**2. REPORT DATE** June 2012	**3. REPORT TYPE AND DATES COVERED** Master's Thesis	
4. TITLE AND SUBTITLE Numerical Study for Optimum Parameters of Bonded Composite Repairs of Cracked Aluminum		**5. FUNDING NUMBERS**	
6. AUTHOR(S) Aaron S. McGee			
7. PERFORMING ORGANIZATION NAME(S) AND ADDRESS(ES) Naval Postgraduate School Monterey, CA 93943-5000		**8. PERFORMING ORGANIZATION REPORT NUMBER**	
9. SPONSORING /MONITORING AGENCY NAME(S) AND ADDRESS(ES) N/A		**10. SPONSORING/MONITORING AGENCY REPORT NUMBER**	
11. SUPPLEMENTARY NOTES The views expressed in this thesis are those of the author and do not reflect the official policy or position of the Department of Defense or the U.S. Government. IRB Protocol number _____N/A_____.			
12a. DISTRIBUTION / AVAILABILITY STATEMENT Approved for public release; distribution is unlimited		**12b. DISTRIBUTION CODE**	

13. ABSTRACT (maximum 200 words)

This thesis used Finite Element Analysis to model a cracked aluminum panel repaired with a bonded composite patch using the minimization of energy release rate in mode I crack growth conditions to determine effectiveness of a patch. The first phase of the study was to understand the mechanics of the effects of asymmetric or one-sided patching for both flat and curved geometries. The out of plane deflection that occurs due to one sided patching had a significant effect. Phase two studied the relationship between patch and base plate stiffness and patch and base plate thickness using orthotropic patch characteristics. Phase two provides general target patch design guidelines that could be used by technicians performing the repair. The third phase studied the effects of varying specific patch design parameters such as patch length and patch width applied to flat plate and curved geometries to provide specific design parameters to use in achieving general patch requirements determined from phase two of this study.

14. SUBJECT TERMS aluminum cracking, numerical analysis, composite patching, curvature			**15. NUMBER OF PAGES** 107
			16. PRICE CODE
17. SECURITY CLASSIFICATION OF REPORT Unclassified	**18. SECURITY CLASSIFICATION OF THIS PAGE** Unclassified	**19. SECURITY CLASSIFICATION OF ABSTRACT** Unclassified	**20. LIMITATION OF ABSTRACT** UU

NSN 7540-01-280-5500

Standard Form 298 (Rev. 2-89)
Prescribed by ANSI Std. 239-18

THIS PAGE INTENTIONALLY LEFT BLANK

Approved for public release; distribution is unlimited

NUMERICAL STUDY FOR OPTIMUM PARAMETERS OF BONDED COMPOSITE REPAIRS OF CRACKED ALUMINUM

Aaron S. McGee
Lieutenant, United States Navy
B.S., University of South Florida, 2006

Submitted in partial fulfillment of the
requirements for the degree of

MASTER OF SCIENCE IN MECHANICAL ENGINEERING

from the

NAVAL POSTGRADUATE SCHOOL
June 2012

Author: Aaron S. McGee

Approved by: Young W. Kwon
Thesis Advisor

Jarema M. Didoszak
Second Reader

Knox T. Millsaps
Chair, Department of Mechanical and Aerospace Engineering

THIS PAGE INTENTIONALLY LEFT BLANK

ABSTRACT

This thesis used Finite Element Analysis to model a cracked aluminum panel repaired with a bonded composite patch using the minimization of energy release rate in mode I crack growth conditions to determine effectiveness of a patch. The first phase of the study was to understand the mechanics of the effects of asymmetric or one-sided patching for both flat and curved geometries. The out of plane deflection that occurs due to one sided patching had a significant effect. Phase two studied the relationship between patch and base plate stiffness and patch and base plate thickness using orthotropic patch characteristics. Phase two provides general target patch design guidelines that could be used by technicians performing the repair. The third phase studied the effects of varying specific patch design parameters such as patch length and patch width applied to flat plate and curved geometries to provide specific design parameters to use in achieving general patch requirements determined from phase two of this study.

THIS PAGE INTENTIONALLY LEFT BLANK

TABLE OF CONTENTS

LIST OF FIGURES

LIST OF TABLES

THIS PAGE INTENTIONALLY LEFT BLANK

LIST OF ACRONYMS AND ABBREVIATIONS

CMAV	Continuous Maintenance Availability
CTE	Coefficient of Thermal Expansion
GUI	Graphic User Interface
MVCCT	Modified Virtual Crack Closure Technique
SERR	Strain Energy Release Rate
SR	Stiffness Ratio
SRA	Selected Repair Availability

THIS PAGE INTENTIONALLY LEFT BLANK

ACKNOWLEDGMENTS

Dr. Kwon, his oversight and guidance was essential to the completion of this thesis. I appreciate the time and patience given to me as I progressed through the learning and research associated with accomplishing this thesis.

THIS PAGE INTENTIONALLY LEFT BLANK

I. INTRODUCTION AND BACKGROUND

A. CG-47 CLASS CRACKING

The CG-47 Ticonderoga Class Cruisers are major warships in the U.S. Navy fleet. The oldest one still commissioned entered service in 1986, nearly 26 years ago. A modernization program was started to extend the lives and effectiveness of the class but the superstructures are experiencing cracking due to sensitized aluminum in the superstructures and in some other areas. Traditional metal repairs such as welding are expensive and difficult to conduct outside of a shipyard environment. There is interest therefore, in the use of bonded composite patches as a repair technique for cracking in sensitized aluminum [1].

Some of the advantages of composite repair that have been experienced in the repair of aircraft, off shore oil production and other naval applications are [2], [3], [4]:

- No Rivet holes causing new stress concentrations
- High stiffness to weight and strength to weight ratios
- The patch can be formed to complex shapes
- Composite materials are resistant to fatigue and corrosion
- Composite repairs are faster than normal metal fabrication repairs
- No requirement for hot work
- Easier in situ repair
- Avoid damage to parent aluminum caused by welding repair
- Easy repair of the patch if it fails

It is the opinion of the author that the use of bonded composite patches to repair structural damage to a Navy ship is well within the capability of ships force. Currently, structural repair must be delayed until at least a scheduled Continuous Maintenance Availability (CMAV) or a full Selected Repair Availability (SRA). In addition, the cost of materials and contractor labor can be prohibitive in a shipyard period. If bonded composite repair is delegated to ship's force, the cost to repair will be reduced to that of the composite material and the time from crack detection to repair could be as little as a day.

B. NAVAL AND MARITIME APPLICATIONS OF COMPOSITE REPAIRS

The Defense Science and Technology Organization (DSTO) for the Royal Australian Navy used large carbon fiber reinforced polymer (CFRP) patches applied to the O2 level deck of their Adelaide Class frigates (U.S. Navy Oliver Hazard Perry Class frigates) to reduce stress concentrations that were causing cracks in mid-ship areas [5]. A 15-year study of the effectiveness of the repair as well as the durability and reliability of the repair showed that repairs using bonded composite materials can be effective and survive in a harsh maritime environment [3]. The design of the repair addressed proper surface preparation, use of the adhesive layer to prevent galvanic corrosion between the CFRP and the base aluminum, use of a Glass Reinforced Polymer (GRP) for environmental protection, and mitigating stress concentrations through stress attraction at the patch edge through the use of ply drop-off. Other important advantages of the CFRP repair over traditional metal repair pointed out in the 15-year study were the price and availability of the materials and labor, no requirement for hot work and only minimal safety precautions associated with the CFRP installation, and the ease at which the patch can be repaired or removed.

Another maritime application of the use of bonded composite repairs is in the oil and gas production industry to repair floating offshore units (FOUs). Repairs have been conducted to repair both fatigue cracking and thinning due to corrosion. Studies conducted on two separate, in service FOUs showed bonded composite repairs to be effective in repairing both types of damage [6].

C. LITERATURE REVIEW

There has been extensive research in the use of composite patches to repair aircraft structures. The following is a summary of engineering and design issues with the use of composite patches in the repair of metallic components.

1. Double-Sided Patches

Applying patches to both sides of a plate containing a crack reduces the stress intensity factor at the crack tip greater than that of a single-sided patch [7], [8], [9]. A single-sided repair causes a shift in the neutral axis away from the center of the host

plate. This induces a bending stress on the plate which is largest on the unpatched surface. This bending stress can significantly reduce the effectiveness of a one-sided repair [10]. The improved effectiveness of double-sided repairs over single-sided repairs has been shown analytically, numerically, and experimentally and show that effort should be made to perform a double-sided repair [8], [7], [11]. However, a double-sided repair will often not be feasible on a ship because the repair area is simply inaccessible and thus will not be considered in this thesis.

2. Patch Design

Some basic considerations in the design of a composite patch are the size, shape, and material used [2]. The size needs to account for proper load transfer from the plate to the patch and deal with any obstructions that may be located in the repair area. It is common to taper the edges of the patch and choose an octagonal shape to reduce stress concentrations at the patch edges and corners [2]. Material considerations are stiffness, coefficient of thermal expansion (CTE) compatibility, and how well the material withstands the operating environment [2]. Common composite materials used in composite repair are E-Glass, Graphite/Epoxy, Boron/Epoxy, and Carbon Fiber composites.

An octagonal shape is a common shape used for the reasons stated earlier as well as being practical for *in situ* repair. However, it was shown by Kumar and Hakeem that a novel skewed shape patch is the most optimum shape patch for double-sided repairs [11]. A skewed patch resembles a bowtie shape with the dimension perpendicular to the crack less than the dimension parallel to the crack. It was found that the skewed shape reinforces more of the high stress area and less of the low stress area resulting in a lower stress intensity factor [11].

The adhesive used to bond the patch to the plate is also a significant factor in patch design. Modified epoxy film adhesives, such as FM-73 are commonly used in the repair of aircraft panels [2]. The size of the patch is important with regard to adhesive effectiveness because enough area, or overlap length, is needed to help minimize shear stresses in the adhesive. A patch length on the order of 80–100 times the thickness of the

repair should be used [12]. The thickness of the adhesive has a limited range of effectiveness between being too porous and weak to too stiff and brittle. This range is typically 0.00489 inches to 0.0098 inches [12]. A thinner adhesive layer was shown to minimize both the stress intensity factor and crack opening displacement, regardless of crack length and patch thickness [9].

Another design factor is the stiffness ratio (SR) of the patched system. The stiffness ratio is defined as $E_{patch}*t_{patch}$ to $E_{plate}*t_{plate}$ where E is the modulus of elasticity and t is the thickness [2], [12]. An accepted range of SR is 1.0 to 1.6. Larger values can cause an increased load attracted to the patched area, or load attraction which would increase the stresses in the adhesive and patch, depending on how much of the load is transferred to the patch [12]. If a higher value of SR is required, the load attraction can be somewhat mitigated by the use of an elliptical patch and adjusting the aspect ratio of the patch as described by Duong and Wang [2].

Composite patch stacking sequence, or patch lay-up orientations, offers significant improvements in fatigue life that can be achieved by choosing an optimal lay-up pattern. Experimental and numerical results were shown to improve fatigue life between 30–85% when compared to non-optimal lay-ups when the crack is in mixed mode conditions [13]. The optimal lay-up combinations in mixed mode conditions were combinations of 90 degrees, 45 degrees, and zero degrees to the crack. If the crack is only in mode I, the orientation that achieves the greatest reduction in stress intensity factor is when the fibers are oriented perpendicular to the crack [14]. The tradeoff in placing a lay-up with all the layers oriented 90 degrees to the crack is the ineffectiveness of the patch if the loading condition changes. A comprehensive numerical study of a cracked plate in mixed mode conditions with a large number of layup options to be combinations of 90 and +/- 45 degree orientations [15].

3. Fatigue Crack Growth

Fatigue crack growth of a cracked panel with a single-sided repair results in a non-uniform crack front through the thickness of the plate [16]. The crack front at the adhesive interface will grow slower than at the free surface end. This difference in crack

front shape is amplified for thick vs. thin plates. A thicker plate means a larger distance between the neutral axis and the free surface, thereby causing the increased crack growth. The non-uniform crack growth is caused by the bending stresses induced by the out of plane deflection and is major reason for the superiority of double-sided repairs over single-sided repairs [17]. For thicker plates, an effectiveness balance or trade-off begins to form between patch thickness and out of plane bending. Numerical and experimental tests have shown that for thick plates, there is a plate thickness in which fatigue life is no longer improved. In the case of a 0.25 inch plate repaired with an E-glass composite patch, increasing patch thickness past eight layers no longer has a significant effect on minimizing fatigue crack growth [17], [18].

4. Thermal Residual Stress

There has been a large amount of work completed investigating the residual thermal stresses using analytical, numerical, and experimental methods [19], [20], [21], [22], [23]. The composite material is required to cure at an elevated temperature and due to a difference in coefficients of thermal expansions (CTE) between the base aluminum and composite patch, significant thermal residual stresses can occur. The CTE of the composite material is much smaller than that of aluminum. When cooling from curing temperatures, the aluminum plate wants to contract more than the composite patch resulting in a tensile traction at the adhesive interface for the aluminum plate countered by a compressive traction for the composite patch. This situation causes out of plane bending and can actually work to close the crack on the free surface, increasing the effectiveness of the patch [21]. Any increase in effectiveness comes at the cost of increased residual thermal stresses and strains.

5. Effects of Plate Curvature

Tong and Sun have conducted extensive numerical investigation of curvature effect on both adhesive stresses and fracture toughness of cracked thin walled structures [24], [25], [26], [27]. The peak peel and shear stresses in the adhesive for both an internally and externally bonded patch subjected to a tensile load with the fixed span increases as curvature increases. However, if the height of the span is fixed, the

adhesive's stresses remain constant. A fixed span test has a changing bending moment whereas a fixed height test does not leading to the conclusion that a bending moment could be a major factor in the peak adhesive stresses [27]. Like adhesive stresses, strain energy release rate (SERR) of a cracked cylindrical structure is affected by curvature when the bending moment changes, either with an applied bending load or with tension load with changing span [25].

Regarding SERR of a cracked cylindrical plate, the work by Tong and Sun was limited to thin shells with externally bonded patches. This thesis seeks to investigate the effect of curvature for a thick curved plate with both internally and externally bonded patches.

D. OBJECTIVES

Composite repair of cracked superstructure panels on a naval vessel present unique loading, plate geometry, and boundary conditions as well as physical constraints on patch placement due to limited access. Plates on the skin of a superstructure typically do not carry a primary load. Loading on a particular plate is unknown but could be characterized as tension due to flexing of the superstructure due to pitch and roll as well as bending if the plate is subjected to some form of load on its surface such as wave impact. Plates on a superstructure are considered to be thick plates. Typically, they are a quarter inch in thickness. Over time, some plates will develop some form or warping due to age and fatigue and should be considered a curved plate as opposed to a flat plate. The thickness of the plate is also a concern due to geometry. It is such that the out of plane bending will occur with a single-sided repair. Therefore, there are two potential sources of bending stresses: the out of plane bending resulting from a single-sided repair and bending resulting from a loaded curved plate.

The goal of this thesis is to investigate the important and relevant parameters in designing single-sided composite patches for thick flat and curved plates using Finite Element Methods. Tension and bending loads will be considered as well as the effects of placing the patch on the inside and outside of the plate curve. Parameters investigated are patch length, width, stiffness, thickness, and stacking sequence. Each parameter will be

tested for flat and curved plates under both tension and bending. A consolidated summary will be provided for each particular case. To the best of the author's knowledge, there has been no comprehensive investigation of composite patch design parameters for thick curved plates.

Three sets of tests will be run to support the objectives of this thesis, all evaluating mode I energy release rate as the parameter indicating patch effectiveness. The first set will evaluate the effectiveness of a patched system for the various loading and boundary conditions as the curvature of the plate is increased. The second set will examine the effectiveness of patches with equal stiffness ratios but different stiffness and thickness combinations. The third set evaluates the effect of patch length and patch width.

THIS PAGE INTENTIONALLY LEFT BLANK

II. MODEL

A. FINITE ELEMENT MODEL

Various finite element models were created using ANSYS Mechanical ADPL Release 13 along with various boundary conditions and various load conditions. The different geometries, load conditions and boundary conditions are used to simulate the many conditions to which a particular plate found on a ship may be subjected.

1. Model Geometry

Figure 1 shows a flat plate model, which was used as a reference model throughout the testing. The flat plate has a center crack of length 2a with length measured perpendicular to the crack and width measured parallel to the crack. The patch is adhesively bonded to the aluminum plate. The patch has a length and width in the same orientation as the plate and angle θ is the orientation of the particular layer of a composite layup. Symmetry is utilized to split the model in half through the width. Plate dimensions are standard throughout with Length = 24 inches, Width = 20 inches, and Thickness = 0.25 inches. Adhesive thickness is also standard throughout and set at 0.01 inches. All other dimensions vary depending on the particular test.

Figure 2 shows the basic geometry for the curved concave plate. Concave is used to describe the free surface of the patch. The geometry in Figure 2 will be referred to as 'concave' throughout this thesis. The patch is curved along the length and is straight along the width. The radii of curvatures investigated are 144.25 inches and 72.5 inches, which represent a depth of 0.5 inches and 1 inch, respectively, for a plate length of 24 inches. The other dimensions are consistent with the flat plate model. This model, like the convex model described next are intended to capture the deformations common on deck and superstructure plating found on older Navy ships.

Figure 3 shows the basic geometry for the curved convex plate. Again, convex is used to describe the free surface of the patch and the geometry in Figure 3 will be referred to as "convex" throughout this thesis. The dimensions and curvatures are consistent with the concave plate model.

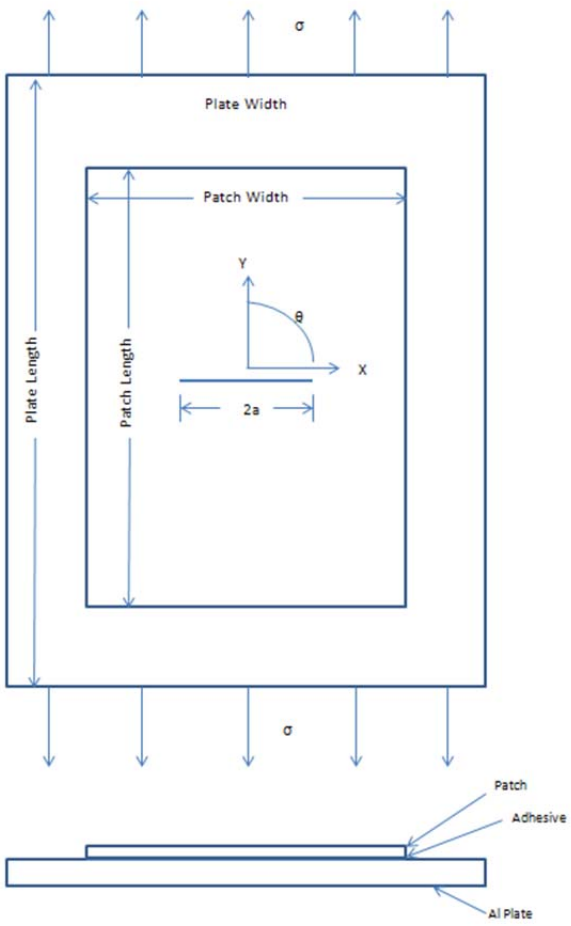

Figure 1. Flat plate geometry

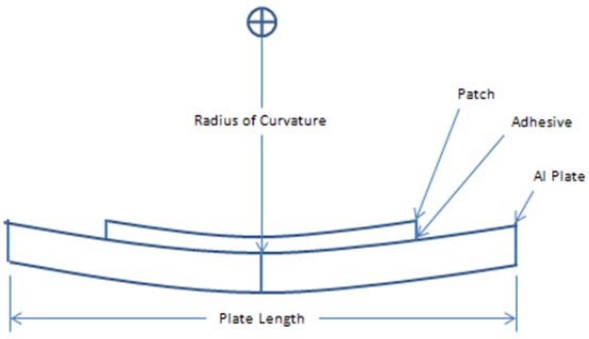

Figure 2. Concave plate geometry

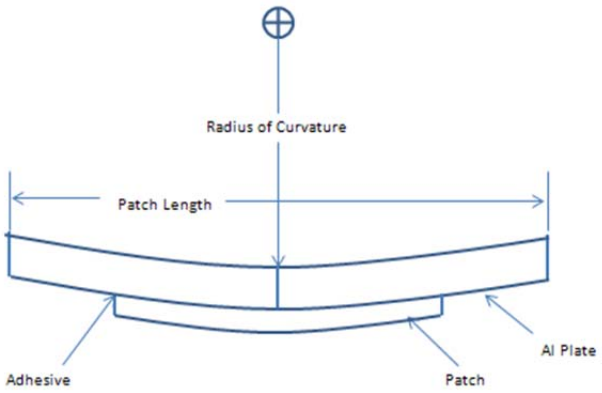

Figure 3. Convex plate geometry

2. Model Construction

Each of the three geometries was constructed using the same solid modeling techniques and elements. Therefore only the construction of the flat plate model will be discussed in detail. The model was constructed using 20-node brick elements (ANSYS element solid186). Four elements were used through the thickness of the plate, the reason for which is discussed in the numeric stability section. Two elements depth through the thickness was chosen for the adhesive layer so the crack opening at the plate/adhesive interface was not held shut on a row of nodes. Figure 4 shows a side view of the deformed system, illustrating the need for at least two adhesive layer elements. Two or three elements were used through the thickness of the patch to avoid hourglass mode by the element [28]. The patch elements were modeled using layered 20-node solid186 elements to simulate the composite material. In parts of this research, the patch was modeled as a homogeneous material and therefore the same homogeneous 20-node solid186 elements used in for the plate and adhesive are used for the patch. Each layered element layer modeled 4 composite fiber layers with varying orientations depending on the particular test. The left image in Figure 5 shows the front view of the flat plate model and the right image is turned slightly on the y-axis to show the extension of the plate. In the image, the left side of the plate is the symmetry plane so what is seen is the right half of the plate and patch.

The thickness of the adhesive layer relative to the other layer is a major source for the poor element aspect ratios. The analysis was conducted without the adhesive layer, and that produced significant inaccuracies in the results. Once included, the change in thickness had only a minor effect on the results of the analysis. A large adhesive layer thickness of 0.01 inches was then chosen to slightly aid in reducing the poor aspect ratios.

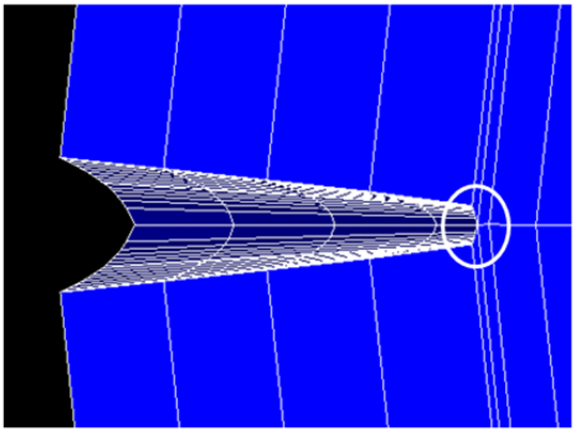

Figure 4. Deformed adhesive elements

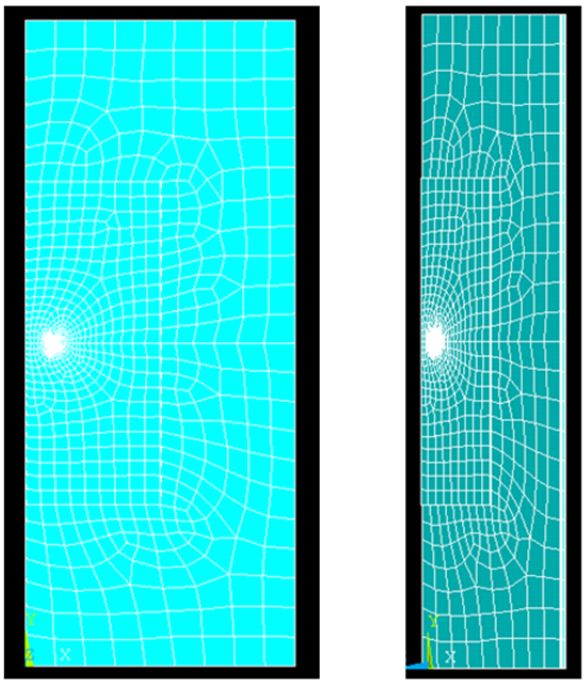

Figure 5. Flat plate model; Left: front view, Right: off axis view

The cluster of elements in the center left section area of the model in Figure 5 is the location of the crack tip and is called the "crack zone." It is cluster of square elements used to ensure equal element lengths along the crack which is required for the Modified Virtual Crack Closure Technique to calculate Energy Release Rate. Figure 6 shows a close up of the front face of the crack zone.

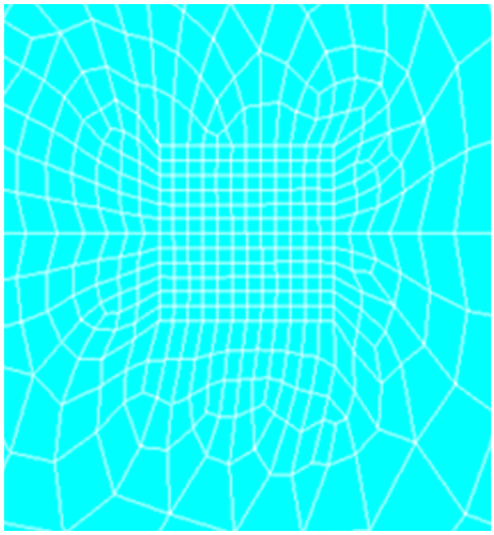

Figure 6. Crack zone; Left: deformed model, Right: undeformed model

The upper and lower crack faces were modeled as contact surfaces using contact174 and target170 contact element pairs. Using contact elements created a non-linear solution and increased the processing time from about 2 minutes to about 10 minutes. The use of contact elements was necessary to properly model the plate under a bending load. In bending, the crack edge on the adhesive surface becomes a fulcrum. So if not modeled as a contact pair, the elements will merge and occupy the same space. The left side of Figure 7 shows the side of the entire model deformed without a contact pair. The space violation by the two crack surfaces can be seen at the adhesive surface. The right side is a close up of just the plate element layer at the adhesive surface. A useful image of a properly modeled deformed crack is not available because of how ANSYS scales deformed shapes, but was verified by obtaining positive values when subtracting the displacements along the length of the plate of the crack bottom nodes from the crack top nodes.

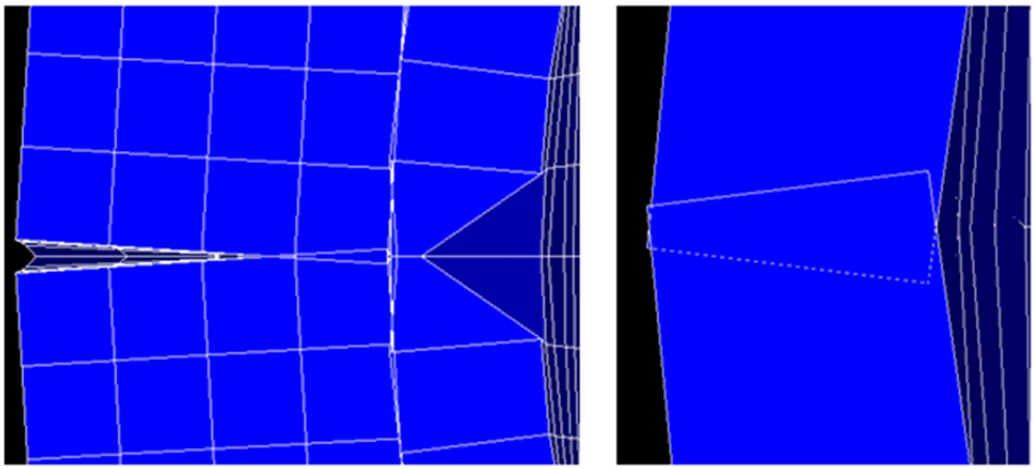

Figure 7. Deformed model without contact pairs; Left: full model, Right: close up view of the aluminum plate elements at the adhesive interface

3. Non-linear Geometric Analysis

The non-linear geometry function in ANSYS was used throughout this research. It was determined that even for small deflections, such as those in a flat cracked plate with a single-sided repair, linear geometric analysis was inadequate; this concurs with the findings of Sun and Chin [29]. Figures 8 and 9 show the deformation of a flat cracked unpatched plate after a pressure of 10 psi was applied to the top surface. Figure 8 is the result of a non-linear analysis and the Figure 9 is a result of linear analysis. Figure 8 shows a smooth even deflection which is what would be expected with the given conditions. Figure 9 is subjected to the same loading and boundary conditions but shows an uneven and unexpected deflection.

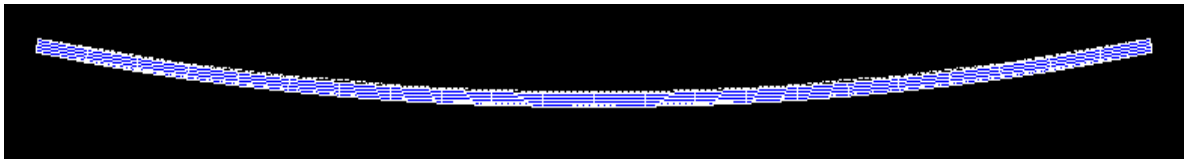

Figure 8. Non-linear analysis of an unpatched flat plate subjected to a pressure of 10 psi

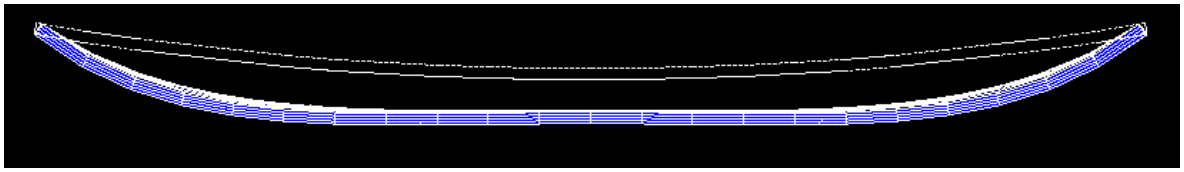

Figure 9. Linear analysis of an unpatched flat plate subjected to a pressure of 10 psi

An additional example of the difference between linear and non-linear analysis is Figure 10, shows how the difference in peak Mode I Strain Energy Release Rate, G1 changes as a function of depth of curvature for an unpatched flat plat subjected to the same boundary and load conditions as above. The non-linear analysis captures a smooth decrease in G1 which indicates a smooth transition in stress state. The linear analysis shows an unrealistically steep increase and then decrease in G1 just as the plate begins to take on a curve.

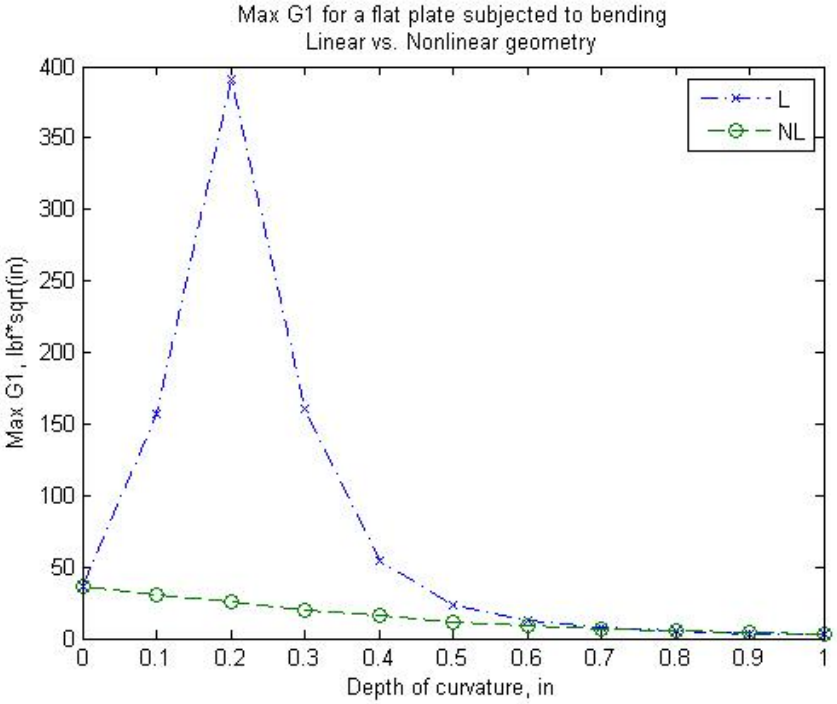

Figure 10. Linear and non-linear geometry G1 for a flat cracked plate subjected to a bending load.

Non-linear analysis is required when non-linearities are encountered in the structure due to large deflections. Further details of non-linear geometry in ANSYS can be found in chapter 3 of the Theory Reference, but is usually required when there is large strain, rotation, or stress stiffening [30]. The change in geometry of the models in this thesis is small, on the order of 0.01 inches and less, but every analysis conducted showed a difference between linear and non-linear analysis. The details of each are not listed in this thesis but the results presented were all obtained using non-linear analysis.

4. Loads and Boundary Conditions

Two basic load conditions were used in modeling. The first was 2000 psi tension perpendicular to the crack applied to the top and bottom surfaces of the plate. The other was a 10 psi pressure applied to the entire face of the plate (or patch and plate system) which was used to simulate a bending condition. The tension load case is shown in Figure 1 and the bending load case is shown in Figure 11.

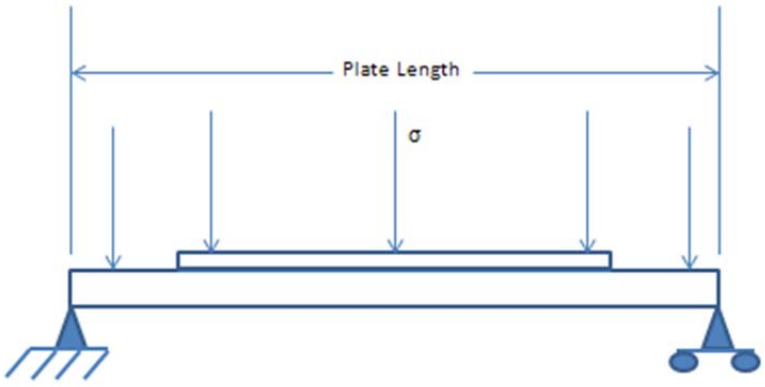

Figure 11. Bending load case

The boundary conditions were designed to support simulation of a standard compact tension and bending test as well as a fully edge constrained plate. Including two different boundary conditions, one with free edges and one fully constrained, provides upper and lower bounds on the effects due to bending. Each plate on a ship is obviously constrained where it is welded to a support. However, a small crack in a large plate may act more like the boundary conditions in Figure 11 whereas a crack in a small plate may act more like the boundary conditions in Figure 12. The boundary conditions in Figure 11 represent those used for both tension and bending. Figure 12 shows the fully constrained plate for bending. When a uniform pressure load is applied to the simply supported boundary conditions seen in Figure 11, it will be referred to as "free bending." The clamped boundary conditions in Figure 12 will be referred to as "constrained bending."

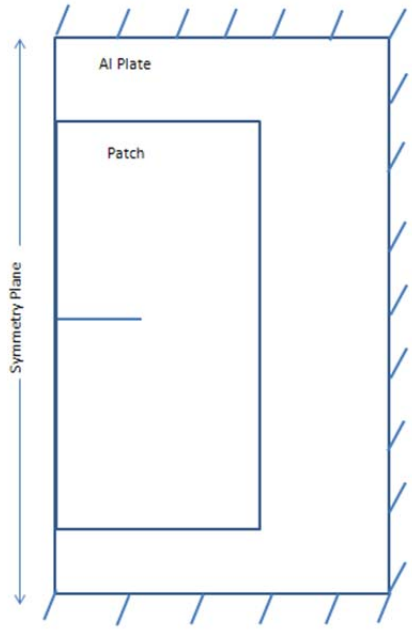

Figure 12. Constrained bending boundary conditions

Due to the volume of data generated and to improve readability, the free bending data will only be included in the body of the thesis when analyzing the change of radius effects. The complete set of results is available in the Appendix for review. The constrained bending case was chosen over the free bending case because it is a better representation of the boundary conditions experienced by the superstructure and deck panels.

B. MODE I ENERGY RELEASE RATE CALCULATION

Mode I Energy Release Rate (GI), or crack opening is the optimization metric used throughout this research. This study assumes no delamination between the patch and the plate occurs; therefore Mode II, crack growth due to plane shear, and mode III, crack growth due to out of plane shear are not considered. Stress Intensity Factor (SIF) and crack growth rate under cyclic loading are other important metrics used in fracture mechanics and both can be calculated starting with the energy release rate. SIF can be calculated from energy release rate using Equation 1 listed below [31]. Equation 1 is for plane stress conditions, which can be modified for plan strain by dividing by $(1-\nu^2)$. The crack growth under cyclic loading can be described using the Paris Law, Equation 2,

where a, N, m, and c are half of the crack length, number of cycles, and material constants. Experimental and finite element data has shown the relationship between energy release and crack extension to be valid for cracked 0.25-inch plates with a bonded composite patch [32], [33], [13].

$$K = \sqrt{EG} \tag{1}$$

$$\frac{da}{dN} = C\Delta K^m \tag{2}$$

1. Modified Virtual Crack Closure Technique

The Modified virtual crack closure technique (MVCCT) is a method to extract Mode I energy release rate from a finite element model and is used in this study. The technique assumes the displacements experienced in front of the crack tip node are equal to the displacements that would occur behind the crack tip node if the crack were to extend. Then assuming that the energy released is equal to the energy it would take to close the crack, the energy released can be calculated by multiplying the nodal forces by nodal displacements along a particular direction and dividing by the area of the element [31]. To use this technique, the mesh in front of and behind the crack should be sufficiently small with each element having equal lengths. The crack zone shown in Figure 6 was created to satisfy these requirements. Equations 4 and 5 are used to calculate the Mode I energy release for corners nodes and mid-side nodes, respectively [31]. The left side of Figure 12 shows the notation for mid-side node calculation and the right side shows the corner node notation. Appropriate terms are excluded from Equation 4 when used to calculate for elements on the edge of the model.

$$G_1 = -\frac{1}{2\Delta L}\left[\frac{1}{2}Z_{Ki}(w_{Kl} - w_{Kl^*}) + Z_{Li}(w_{Ll} - w_{Ll^*}) + Z_{Lj}(w_{Ml} - w_{Ml^*}) + \frac{1}{2}Z_{Mi}(w_{Ml} - w_{Ml^*})\right] \tag{3}$$

$$G_1 = -\frac{1}{2\Delta L}\left[\begin{array}{l}\frac{1}{2}Z_{Li}(w_{Ll} - w_{Ll^*}) + \frac{1}{2}Z_{Lj}(w_{Lm} - w_{Lm^*}) + Z_{Mi}(w_{Ml} - w_{Ml^*}) + \ldots\ldots \\ \ldots\ldots + \frac{1}{2}Z_{Ni}(w_{Nl} - w_{Nl^*}) + \frac{1}{2}Z_{Nj}(w_{Nm} - w_{Nm^*})\end{array}\right] \tag{4}$$

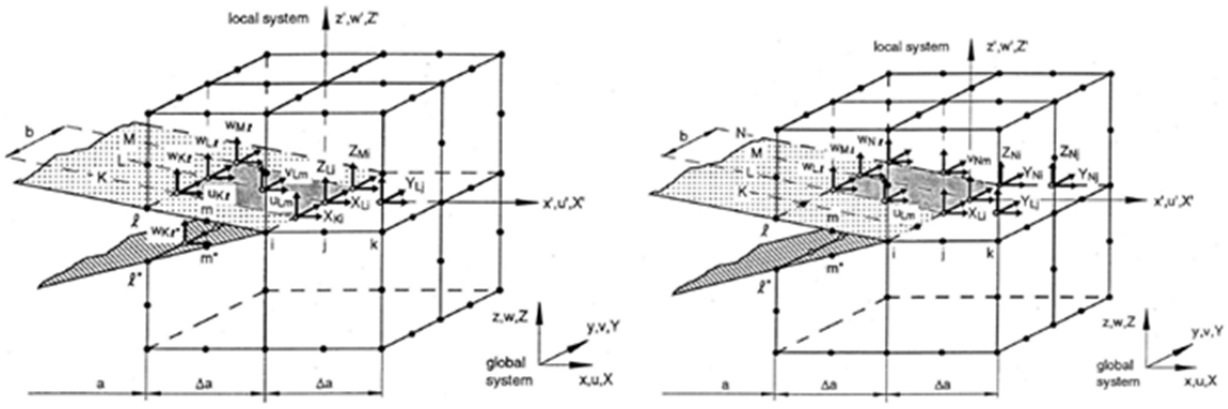

Figure 13. MVCCT notation reference. Both images from [33].

ANSYS has the functionality to calculate the energy release rate for modes 1–3 as total energy release. For ANSYS Release 13, this function only works with the solid186 20 node element when using the ANSYS graphic user interface (GUI). However, a known software deficiency causes ANSYS to terminate a program if this function is called while running in batch mode [34]. Batch mode was essential due to the number of simulations run to support this research. A series of programs were written to extract the relevant nodal forces and displacements from the crack front and then implement Equations 3 and 4.

C. MODEL VERIFICATION

Due to the thickness of the adhesive layer, large aspect ratios are unavoidable unless mesh sizes is minimized throughout the model resulting in a computationally inefficient and time consuming model. The ANSYS Preconditioned Conjugate Gradient iterative equation solver (PCG) is better at handling ill-conditioned problems, such as those with high aspect ratios and contact elements, and is used throughout this study. To test numeric stability, a series of simulations were run ranging the size of the meshing in the crack zone and in mesh away from the crack. The change in calculated energy release rate was negligible.

To verify model accuracy, simulations of an unpatched crack plate of length = 15 inches, width = 20 inches, thickness = 0.25 inches and with a 2-inch center crack were run and the results were compared against analytical solutions of 0.803 lbf*sqrt(in) for

plane stress and 0.882 lbf*sqrt(in) for plane strain. The accuracy was insensitive to changes in mesh sizes both near and far from the crack as well as plate thickness. However, accuracy improved with the number of divisions, or planes of elements used through the thickness of the plate. Using four planes of elements through the thickness produced a 17% error. The percent error steadily decreased until 20 divisions were reached. Figure 14 is a graph of Mode I energy release rate through the thickness calculated by ANSYS and the horizontal lines show the plane stress and plane strain analytical solutions. The left side shows 10 divisions through the thickness and the right side shows 20 divisions through the thickness.

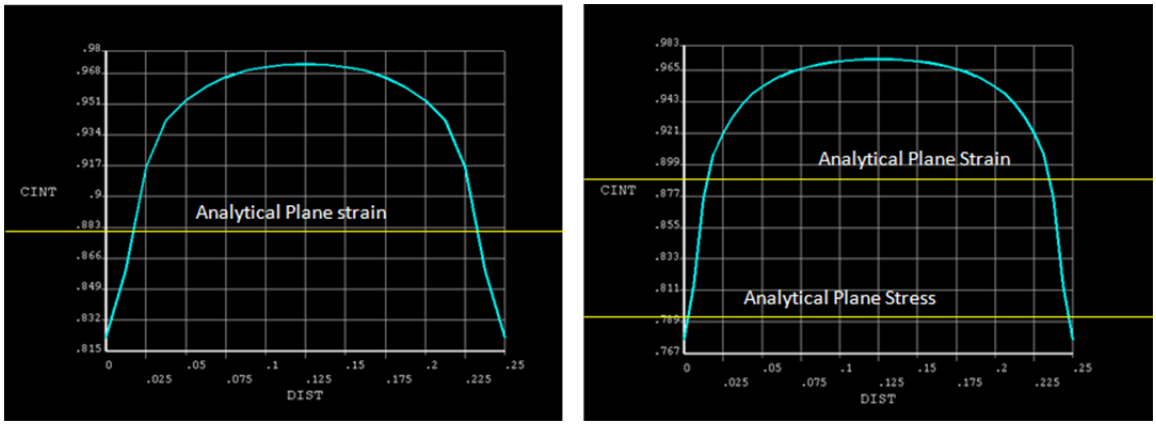

Figure 14. Compact tension test accuracy. L = 10 elements ; R = 20 elements

This study is focused on the energy release rate of a patched system compared to the energy release rate of an unpatched system or a patched system with different patch parameters. Therefore relative values of energy release rate were more useful than absolute. The large number of simulations conducted as part of this study made simulation times greater than 20 minutes unrealistic. With those considerations, the plate was meshed with 4 elements through the thickness.

III. TEST RESULTS AND DISCUSSION

A. OVERVIEW

The test results and discussion are separated by the geometry of the host plate instead of loading conditions or type of test. The reason for this grouping is that the geometry of the plate and which side the patch is to be placed are the constraints by which a patch should be designed. So, the results and discussions are grouped to present the complete set of data for a given plate.

The testing is set up to answer six questions directly.

- Is the system more in bending or tension?
- What is the best general size of patch?
- What is the impact of crack size?
- How well will the addition of a patch decrease G1?
- What is the important geometric parameter?
- What is the impact of clamped edges on the plate?

To improve the readability of this thesis, individual results will only be included in the body of this thesis when they offer additional information not apparent in the constant SR series of tests. A complete set of results are available in the Appendix.

1. Change in Radius Description

The first tests conducted changed the radius of curvature for each particular geometry from a flat plate to a curve of radius 72.5 inches, which corresponds to a depth of curvature of 1-inch for a 24-inch long plate. The objective was to investigate if and how the energy release rate changed as the plate becomes more curved. For ease of visualization, the curve of the plate is given as depth at the center of the plate, zero indicates a flat plate, 0.5 inches corresponds to a radius of 144.25 inches and a depth of 1-inch corresponds to a radius of 72.5 inches.

2. Constant Stiffness Ratio

The stiffness ratio (SR), as described in the literature and shown in Equation 5, is a measure of stiffness of the patch relative to the stiffness of the plate. If the patch is too stiff, then it will cause loads to be attracted to the patched area. If SR is viewed as a design constraint, then the design of the patch has two additional degrees of freedom, the Young's modulus and thickness of the patch. The constant SR test assumes a SR = 1 and varies the patch from a low Young's modulus and thick patch to a high Young's modulus and thin patch, or a thick/soft patch to a thin/stiff patch.

$$SR = \frac{Et_{patch}}{Et_{plate}} \qquad 5$$

The test was run for four different situations using the standard plate dimensions. Plates with crack lengths of 2 inches and 10 inches repaired with patch sizes of 12 inches X 10 inches and 22 inches X 19 inches. The small patch satisfies the minimum size requirements for proper load transfer listed in the literature review and the large patch extends to near the end of the plate. The small patch still covers the large crack by one inch on each side of the crack. The four conditions can be summarized as:

- Small crack / small patch
- Small crack / large patch
- Large crack / small patch
- Large Crack / large patch

When applying the constant SR test to the curved plate geometries, each complete set of tests will be run for a depth of curvature of 0.5 inches and then repeated for a depth of curvature of 1 inch. Running each test as a function of changing radius would be too computationally costly, so two different curvatures were chosen. A 1-inch depth of curvature is an extreme case, and the half inch depth of curvature the more likely case.

The Young's modulus of the patch and corresponding thickness are listed in Table 1. The values for the Young's Modulus were chosen to represent the low end of the E-

Glass up to boron/Epoxy. To achieve a SR of 1 with the host aluminum plate (E_{plate}=10E6 psi, t_{plate} = 0.25 inches), the patch thickness was chosen to satisfy $E_{patch}*t_{patch}$ = 2.5E6.

Table 1. Constant SR test values

	Test 1	**Test 2**	**Test 3**	**Test 4**	**Test 5**
E_{patch} (x10^6 psi)	6	12	18	24	30
t_{patch}(in)	0.4167	0.2083	0.1839	0.1042	0.0833

The output of the test is G1 and out of plane displacement. The plots for G1 are included in the body of this thesis and the values of out of plane displacement are available in the Appendix.

The goal of the constant SR test with two different crack lengths and patch sizes is to investigate how a patched system performs in the many geometries and loading conditions. It should give insight into what is the most important parameter for a given geometry, load condition and crack size.

A secondary conclusion that could be interpreted from the results is an estimate on to what degree the patched system is under tension or bending. Stiffness in tension is Et whereas stiffness in bending is Et^3, again where E is the Young's modulus and t is the thickness. If a system is in pure tension, such as in a double sided repair subjected to a tension load, then the stiffness ratio is defined by Equation 5. However, if the system is in pure bending, then a SR for bending would be defined as Equation 6.

$$SR_{bending} = \frac{Et_{patch}^3}{Et_{plate}^3} \qquad 6$$

The reality of a single-sided repair, regardless of the geometry or loading, is that it will probably be in a condition that lies somewhere between pure tension and pure bending. It is important to understand this relationship because it will determine the

influence of patch thickness over the Young's modulus. A new formula for the stiffness ratio of a system is proposed in Equation 7. For Equation 7, as n approaches one, the system would be more in tension, and as n approaches 3, the system would be more in bending.

$$SR_{mixed} = \frac{Et^{n}_{patch}}{Et^{n}_{plate}} \qquad 7$$

With regard to the constant SR test, a value for n cannot directly be obtained from the results. However, an estimate of where n would lie can be obtained by looking at the ratio of the G1 for test 1, which is a soft patch that is very thick and the G1 for test 5, which is a very stiff and very thin patch. Again, the patch thicknesses in the test were designed using Equation 5 and setting SR = 1. So, if the system being tested was in a state of pure tension, then the results of the constant SR test would show a consistent value for G1. But if the system were in pure bending, where patch thickness should be determined using Equation 6, the values of G1 obtained from the constant SR test would show a significant difference for the varying patch stiffness/thickness combinations. Using the difference in resulting G1 values is not a quantitative measure, but a small difference between test one and test 5 indicates a system more in tension whereas a large difference indicates a system more in bending.

A method to determine an exact value for n is proposed here.

- For a given load case, pick two of the patch Young's modulus. Using an FEA program, determine the value of G1 for the first choice of Young's modulus and any value of thickness.
- For the second choice of Young's modulus, run a series of FEA simulations in which the thickness is varied.
- Plot the values of G1 for the second Young's modulus, and find the thickness that corresponds to the G1 determined for the first Young's modulus case.
- Now with E_1, E_2, t_1, and t_2 determined, equation 7 can be used to determine a value for n for that given load case and geometry.
- This may be repeated for different values of Young's modulus for additional verifications.

Preliminary results for this method were shown to be accurate for single-sided repair of a flat plate under tension where a value of n = 1.6042 was determined. Multiple patches designed according to Equation 7 were tested resulting in a value for G1 within an error of 5%.

3. Varied Dimensional Parameter Description

In the third set of tests, patch length and patch width are varied from minimum to maximum size in each dimension to determine any effect patch dimensions have on the energy release rate of the standard plate models. Excluded from the dimensional parameter test is the patch stacking sequence. Also described in the literature review is the optimal sequence of 90, 45 and zero degrees when a plate is in mixed mode condition. The loading conditions on a superstructure plate are unknown and likely vary dramatically due to things such as sea-state and diurnal heating and cooling. Therefore, based on the work described in the literature, a stacking sequence of 90, 45 and zero degrees is recommended.

For the varied dimensional parameter tests, the plate size is the standard plate size shown in Figures 1–3. The default patch length is 12 inches and the default patch width is 10 inches, or half of the plate for each dimension. The patch is modeled as a 12-layer E-glass patch with material properties listed in Table 2 and a layup of $[90\ 45\ 135\ 0]_3$ relative to the crack.

Table 2. E-glass patch properties

	E_x	E_y	E_z	ν_{xy}	ν_{yz}	ν_{xz}	G_{xy}	G_{yz}	G_{xz}	Ply thickness
psi	7.252E6	2.103E6	2.103E6	0.33	0.33	0.33	3.713E5	3.249E5	3.713E5	0.012 in

B. UNPATCHED PLATE CHANGE IN RADIUS

Prior to analyzing the patched systems, the following is a quick look at the energy release rate of a cracked plate subjected to a bending load. The left plot in Figure 15 is for a constrained plate and the right image is for a plate with free edges.

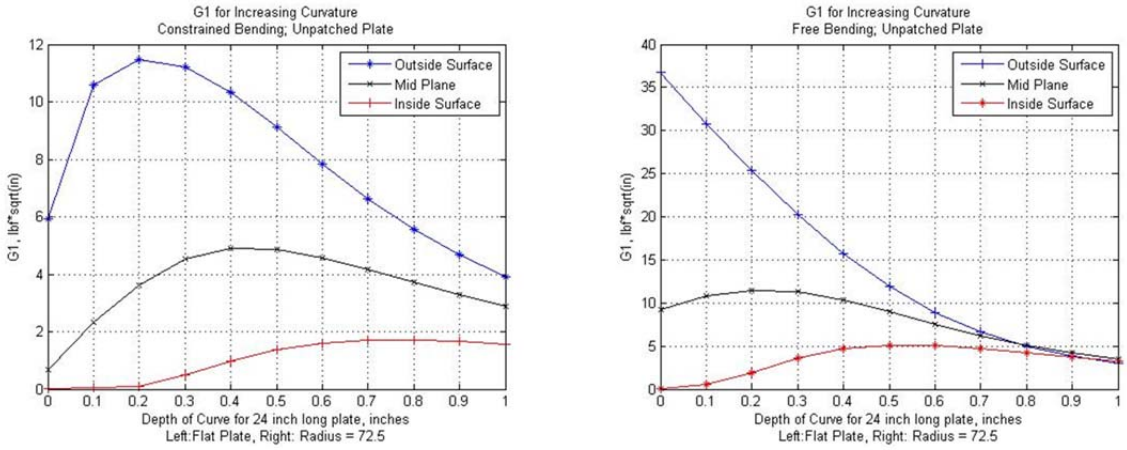

Figure 15. G1 for an unpatched plate, Left: constrained bending, Right: free bending

In both cases, the higher values of G1 occurred when the plate was only slightly curved and the values for G1 through the thickness of the plate are quite different. As the curve of the plate was increased, the values of G1 decreased and became more uniform through the thickness. The free bending case shows, by noting the difference in G1 values, how the plate starts out initially in a bending condition. There was a large difference in G1 occurring through the thickness of the plate, the largest occurring on the side opposite of the load. But as the plate became more curved, the values of G1 converged to the same value, which is what would be expected for a plate under tension. This showed the transition from a non-uniform bending condition to a uniform bending condition.

The actual true condition probably lies somewhere between the two boundary conditions. Visually interpolating the data between the two plots in Figure 15, it is noted that under a bending load, the highest values of G1 are when the plate just begins to curve. A maximum value of G1 occurs at or before a depth of curvature of 0.3 inches

(radius = 240.15 inches). Once the maximum is achieved, the value of G1 decreases and begins to approach a uniform value through the thickness.

C. FLAT PLATE RESULTS

The entire set of data for the flat plate geometry can be found in Figures 44-58 in the Appendix. Only the plots showing the worst case patch performance are included in the body of the thesis.

There are two geometries investigated in the Flat Plate series of tests. Referring back to side view in Figure 1, the patch could either be placed on the top or the bottom of the plate. Or in reference to an applied load on the face of the plate, the bending load could be applied to the patch or the unpatched side. The change in radius test does not apply to flat plate geometry.

1. Tension

It is shown in Figures 16 and 17, that the system is only slightly in bending for a small crack but is more in bending for the larger crack. Again, a difference in G1 between the first and last test cases is an indication of bending. Another simple observation is that G1 increases with larger crack size, as expected.

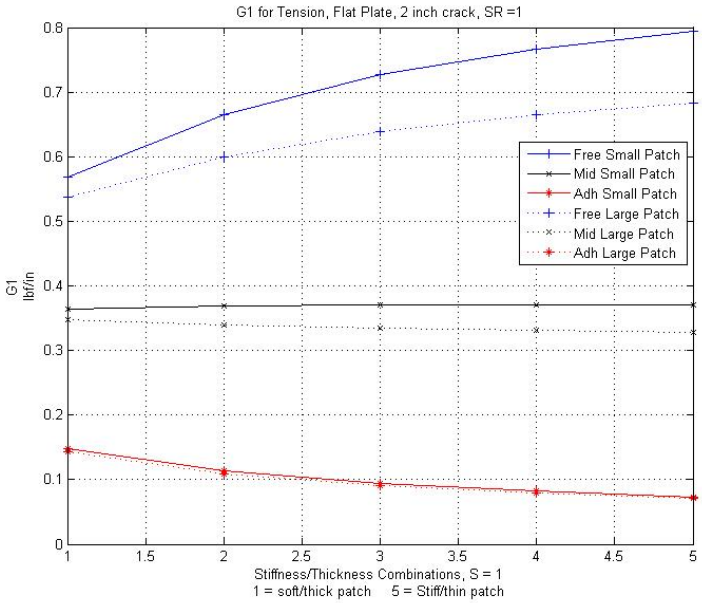

Figure 16. Constant SR, flat plate, tension, 2-inch crack

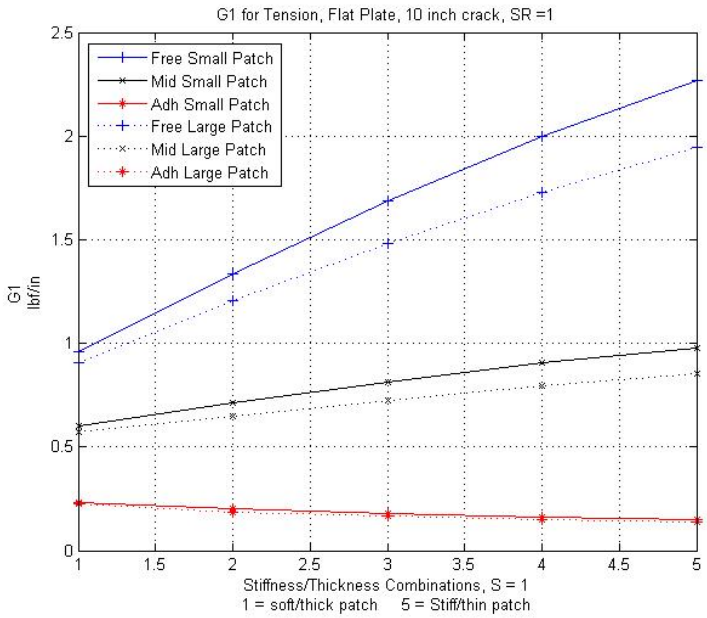

Figure 17. Constant SR, flat plate, tension, 10-inch crack

An interesting observation is in relating the optimal patch size compared to the out of plane displacement. Figures 16 and 17 clearly show that a larger patch is more effective. However, Figure 18 shows that the larger patch size causes a greater out of plane displacement. It is widely reported in the literature that increasing the out of plane displacement causes the crack to grow more, especially in thick plates [17]. Even though a larger patch causes more out of plane displacement, it is more of a global displacement of the entire plate instead of localized around the crack. This results in a smoother curve which reduces the bending effect at the crack tip. Figure 19 shows the impact of increasing patch length on patch effectiveness. It is clearly shown that the patch becomes more effective with increased length. An important observation of Figure 19 is that a patch that is too short will actually cause an increase in G1 over an unpatched plate. Regarding patch width, Figure 44 in the Appendix shows patch width as a non-critical parameter.

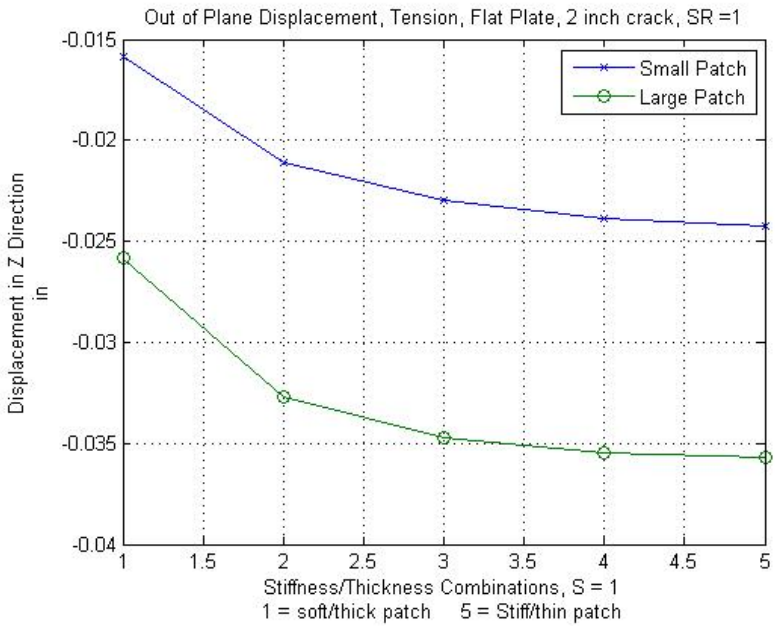

Figure 18. Constant SR, flat plate, 2-inch crack, out of plane displacement

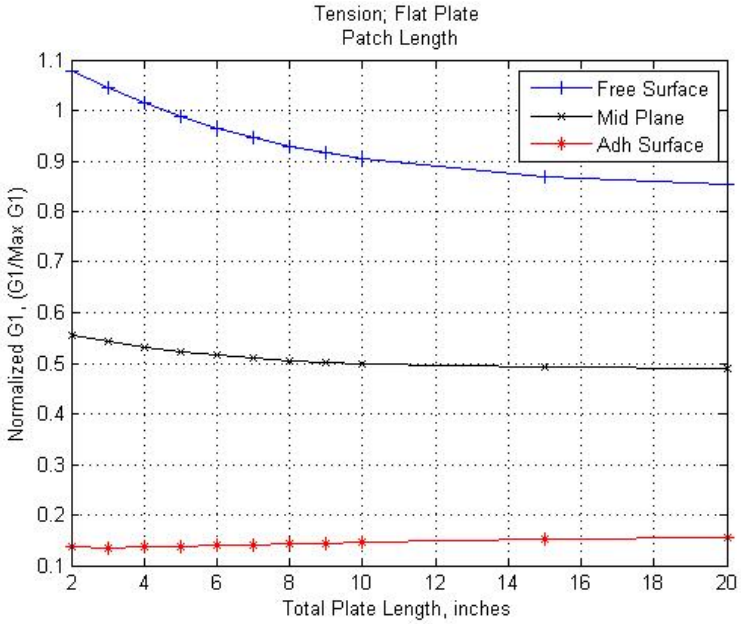

Figure 19. Flat plate, tension, vary patch length

2. Bending with Load Applied to the Patched Side

Figures 20 and 21 both show the resulting G1 for constrained and free bending condition on a flat plate with a two inch crack. One notable observation is the difference

in magnitude between each case which suggests that a clamped boundary has a significant effect on crack growth. Another observation is the amount of bending present in the each system. The free bending system has a much larger degree of bending than the constrained bending system. This result is very intuitive and explains the large difference in magnitudes between the two systems. Interpreting this and applying it to shipboard applications, it means that a bending load applied to a cracked plate with a crack tip far from the welded edge of the plate is much more significant than if the crack tip were close to the edge.

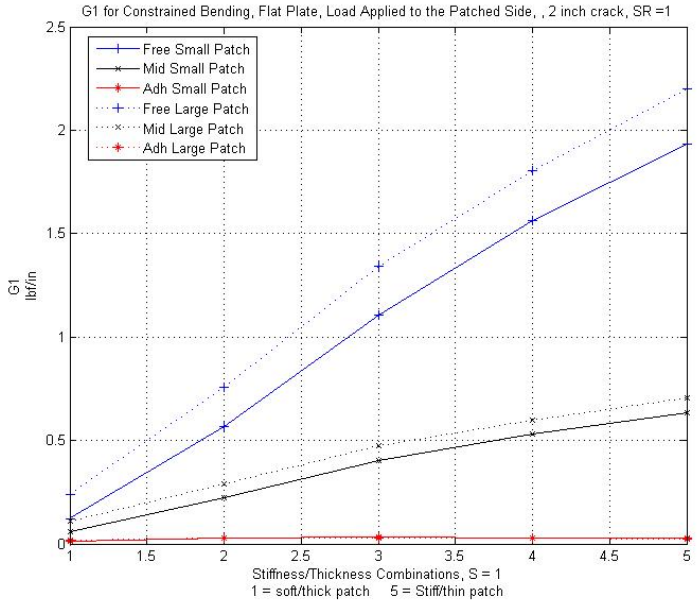

Figure 20. Constant SR, flat plate, constrained bending with patched side loading, 2-inch crack

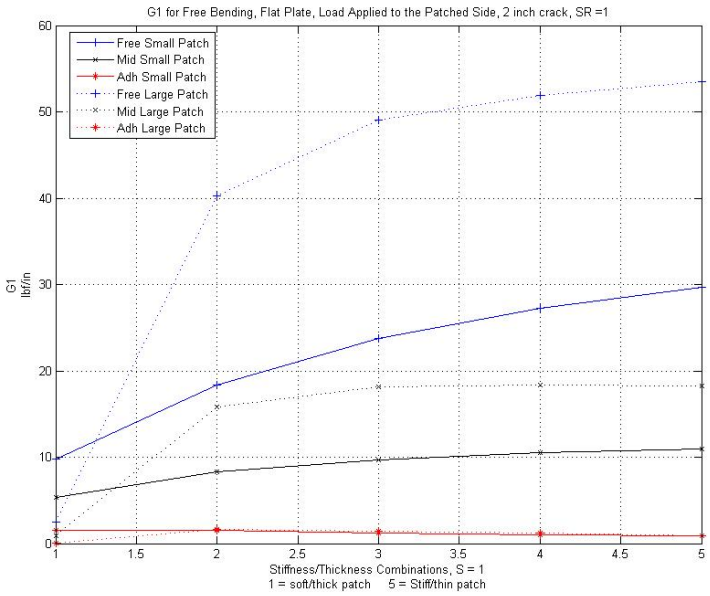

Figure 21. Constant SR, flat plate, free bending with patched side loading, 2-inch crack

With regard to the patch size, Figure 20 clearly shows that a larger patch is more effective in a constrained bending condition. Figure 21 shows a change in effectiveness between the two patch sizes for the different tests. This is an indication that the optimum patch size may also be a function of the stiffness ratio. The data is therefore considered inconclusive. To determine the optimum patch size for this condition, the E*t combinations would need to be re-designed using SR_{mixed} (Equation 7).

The optimum size of the patch for the tension and the constrained bending load contradict each other. To determine which load case should be considered the critical design load case, the effectiveness of patching in each case needs to be compared. Referring to Figures 44 through 48 in the Appendix, the range of values for G1 normalized to the unpatched system for the two cases are:

- Tension: 1.1 – 0.85 (ineffective – 15% reduction in G1)
- Bending: 0.6 – 0.4 (40% – 60% reduction in G1)

Based on the range of the normalized G1 values, the critical load case for a flat plate is tension.

3. Bending with Load Applied to the Unpatched Side

The reduction of G1 for a bending load applied to the unpatched side of a flat plate is very large. Figure 22 shows the varied dimensional parameter test with the least effective patch. The least effective situation still reduces G1 by as much as 91% when compared to the unpatched plate. This suggests the patch is carrying the majority of the load. What can be interpreted is that the addition of even a small and ineffective patch will significantly reduce G1 when there is an applied bending load. This means that when designing a patch for a flat cracked plate on the side opposite of where a bending load would be applied, (such as on the opposite side of a plate subjected to wave loading), the minimization of G1 as a design objective should shift to the other load case and the patches ability to handle the applied bending load should be considered as a design constraint. The remaining figures for this case are excluded from the body of the thesis but are available in the Appendix.

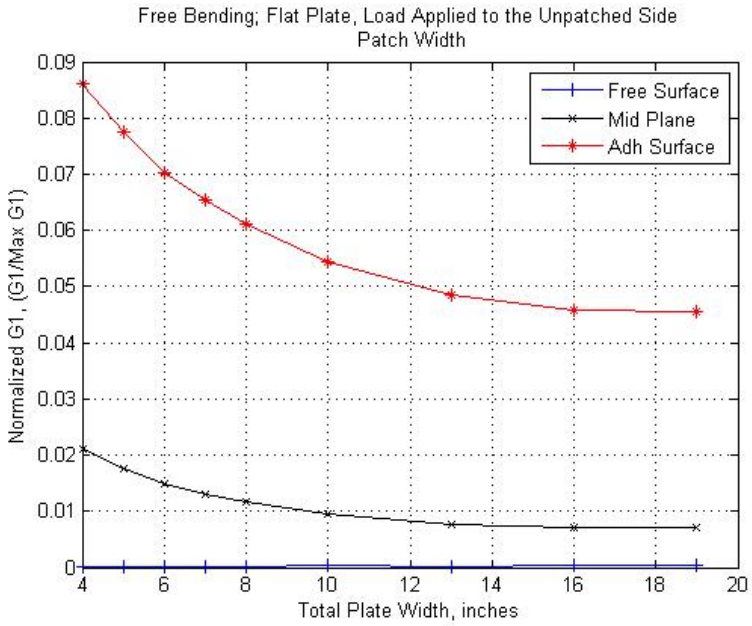

Figure 22. Flat plate, free bending with load applied to the unpatched side, vary patch length

4. Flat Plate Summary

When designing a patch for a flat plate, the critical load case to be analyzed is tension and the important dimensional parameter is length of the patch perpendicular to the patch. If the patch is too short, it may actually increase the rate at which the crack grows. When considering a potential bending load, such as a foot traffic or wave loading, the preferred side on which to place the patch is opposite of where the expected load would be applied. If this can be achieved, then the patch should be designed so it can absorb the entire expected load. If patching on the opposite of the applied load is not possible due to accessibly constraints, it can be considered that a patch designed to optimize the tension load case will be effective in reducing G1 under a bending load.

D. CONCAVE PLATE

The entire set of data for the concave plate geometry can be found in Figures 59 - 76 in the Appendix. Only the plots showing the worst case patch performance are included in the body of the thesis.

1. Concave Plate Change in Radius

In tension, the deflection of the concave plate will try to push itself into the patch. Figure 23 shows that, as the curvature develops, the adhesive surface is trying to pull apart and the free surface of the plate is being pushed together, acting like a fulcrum. The bending case, as shown in Figure 24, has the same shape as the bending of an unpatched plate. Comparing Figure 24 with Figure 15 shows the effect of the patch reduces the magnitude of G1 and shifts the transition from non-uniform bending to uniform bending to a larger curvature.

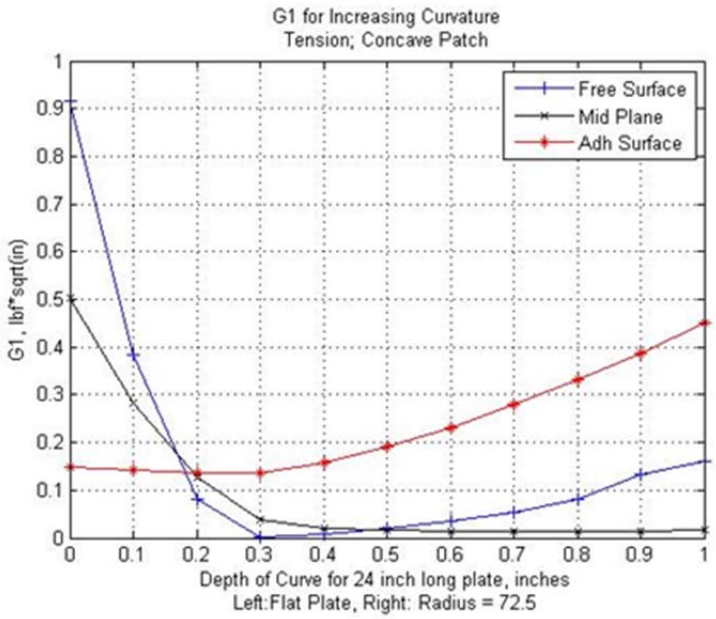

Figure 23. Change in radius, concave plate under tension

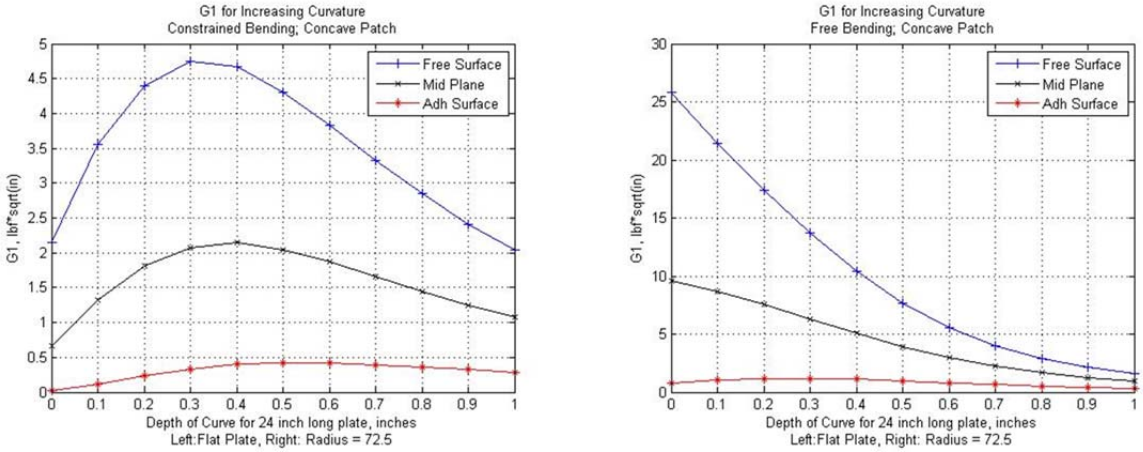

Figure 24. Change in radius, concave plate under bending

2. Concave Plate, Half-Inch Depth of Curvature

a. Tension

The concave test case, like the flat plate unpatched side loading, is not a significant load case to consider for reducing G1. Figure 25 shows the varied dimensional parameter test with the least effective patch. A poorly designed patch will still be over

90% effective in reducing G1. Therefore, when designing a patch for a concave plate, the parameters to minimize G1 should be shifted to the bending case. The ability of the patch to handle the expected tension load should be considered a design constraint.

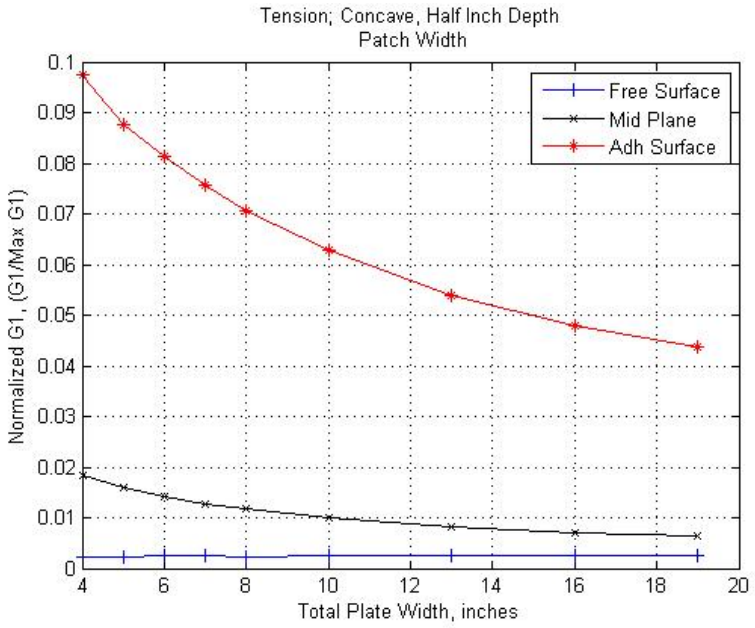

Figure 25. Concave plate, tension, 0.5-inch depth, vary patch width

b. Bending

Figures 26 and 27 show the results for constrained and free bending of a curved plate of 0.5-inch depth for the two different crack sizes. It can be seen that the system in constrained bending conditions is more in a state of bending whereas the system in free bending conditions is more in tension. Furthermore, the differences seen by increasing the patch size are small and contradict each other between the two different boundary conditions. A larger patch is better in constrained bending conditions where a smaller patch is better in free bending. The 10-inch crack data, Figures 70 and 74 in the Appendix, both show that a larger crack has little effect with the constrained bending but nearly doubles the G1 values for the free bending condition.

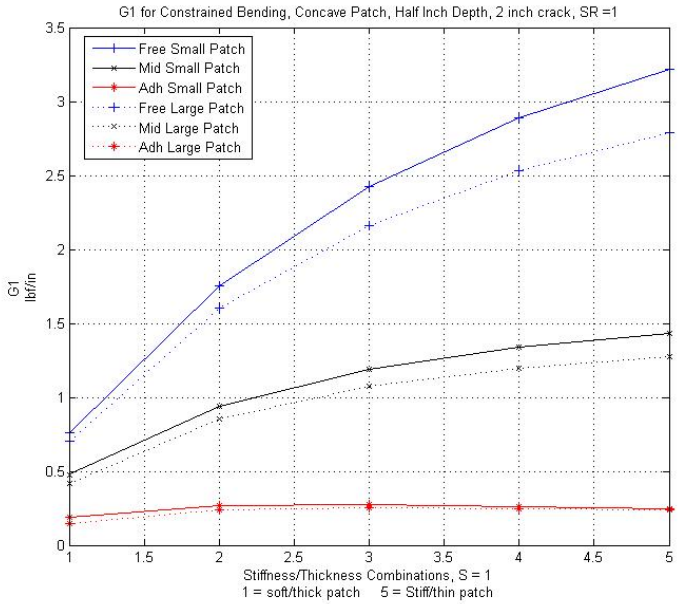

Figure 26. Constant SR, concave plate, 0.5-inch depth, constrained bending, 2-inch crack

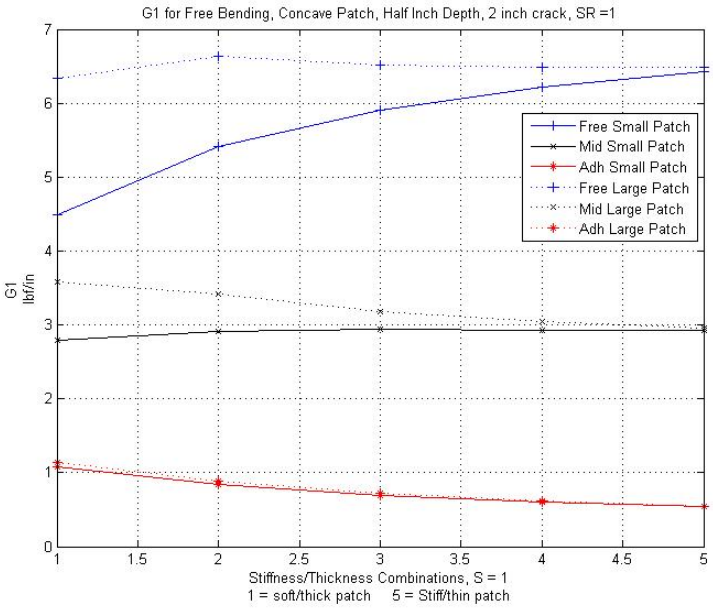

Figure 27. Constant SR, concave plate, 0.5-inch depth, free bending, 2-inch crack

It is difficult to determine what the optimal size for a patch on a 0.5-inch depth curved plate based on the constant SR test data should be. The varied dimensional parameter tests provide more insight. Figure 28 shows the patch length test and shows a

small increase in patch performance as the length is increased, eventually reaching a plateau at about the 10-inch point, or half way across the plate. The entire set of varied dimensional parameter data can be found in the Appendix, Figures 61–66, and show similar curves. For free bending conditions, performance ranges from five to 12 percent whereas there is a 20–30% reduction in G1 for a constrained bending case.

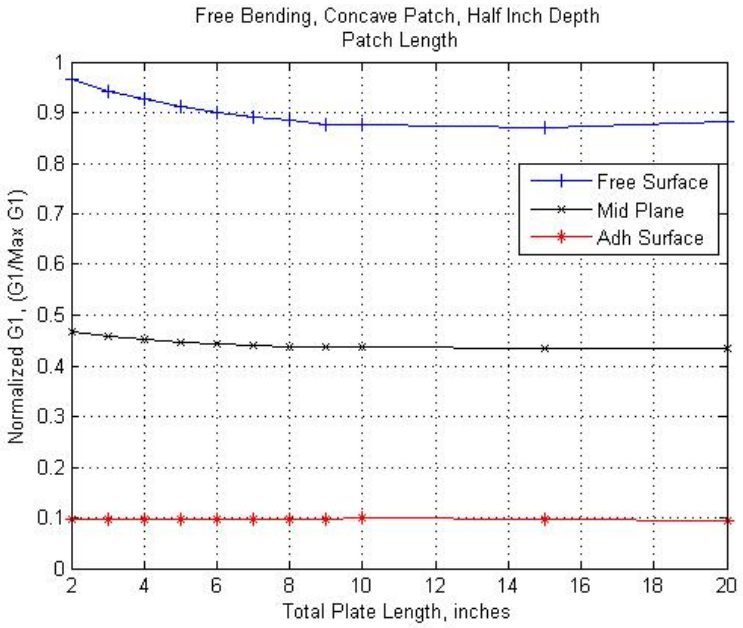

Figure 28. Concave plate, free bending, 0.5-inch depth, vary patch length

3. Concave Plate, 1-Inch Depth of Curvature

a. Tension

The results for a concave plate with a 1-inch depth of curvature indicate the same conclusions as previously discussed for the 0.5-inch depth of curvature. Therefore bending should be considered for minimization of G1 and tension should be considered as a design constraint.

b. Bending

The constrained bending case for a concave plate with a 1-inch depth of curvature is shown in Figure 29. Referencing the complete set of the constant SR test data

in the Appendix, it can be seen that there is little difference between the 0.5-inch depth and 1-depth concave plates. The only notable difference is a decrease in G1 for the plate with greater curvature.

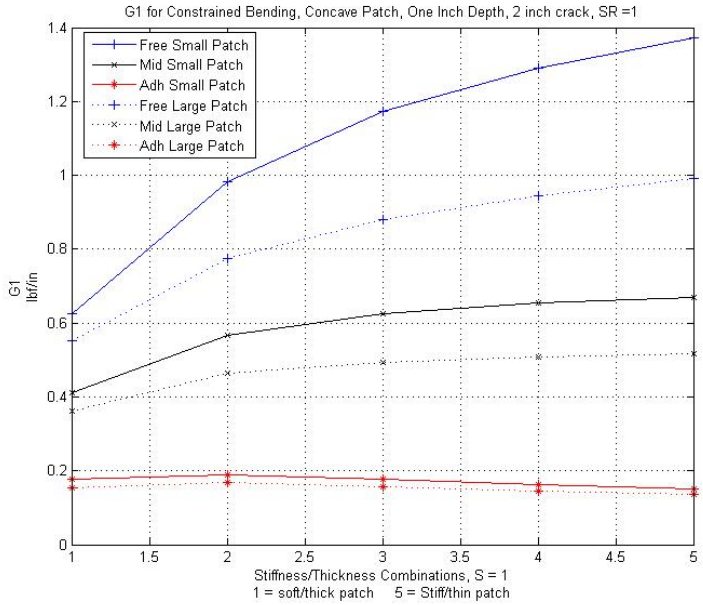

Figure 29. Constant SR, concave plate, constrained bending, 2-inch crack

The varied dimensional parameter data again provides some insight into an optimal patch size. Figure 66 in the Appendix show that varying the width has little effect once the patch extends 2–3 crack lengths past the crack tip. However, Figures 30 and 31 both show patch length as a much more important parameter. In both conditions, the longer patch performs better. In constrained bending, the increase in performance is steady reaching a maximum 25% improvement. The improvement of patch performance in the free bending case is more dramatic and then reaches a maximum of just over a 30% improvement when the patch reaches about 2/3 of the plate length.

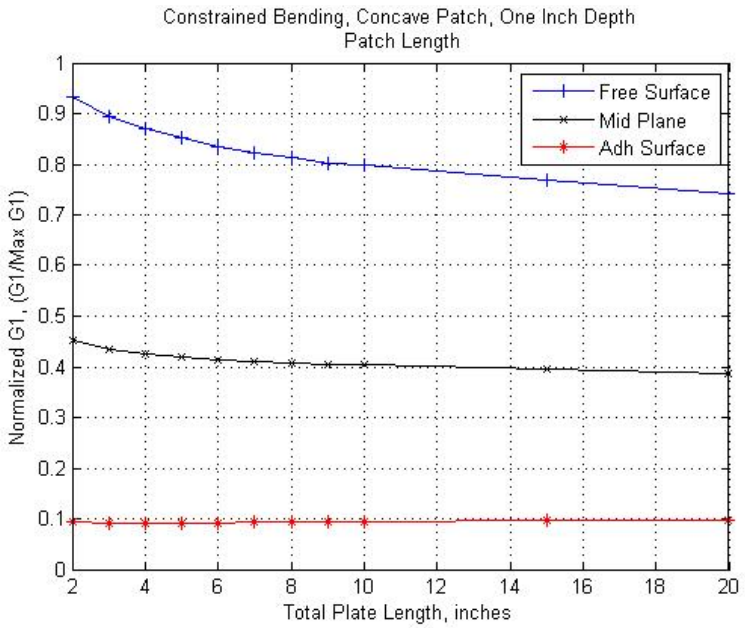

Figure 30. Concave plate, constrained bending, 1-inch depth, vary patch length

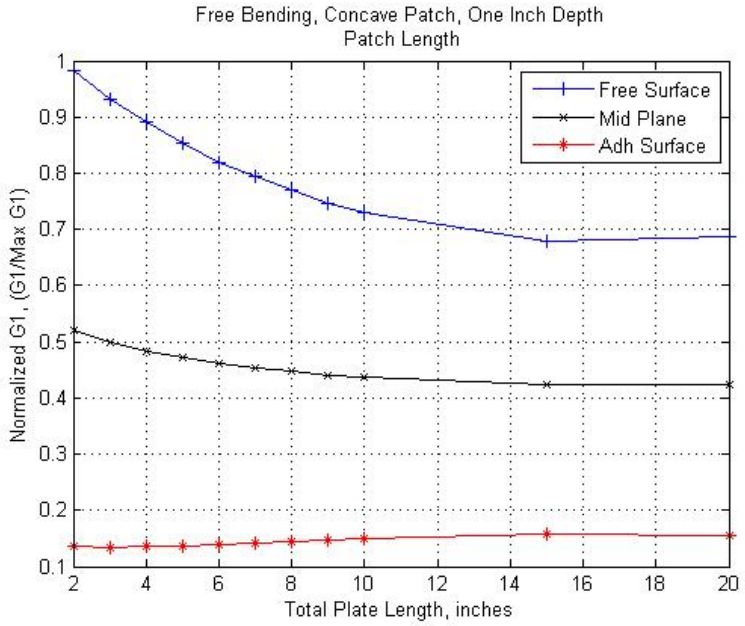

Figure 31. Concave plate, free bending, 1-inch depth, vary patch length

4. Concave Plate Summary

When designing a patch for a concave plate, the critical load for optimal design is bending and the patch length is the critical dimensional parameter. Patch performance also increases with curvature. For the 0.5-inch depth curved plate, the advantage gained by increasing the length eventually reaches a plateau whereas the patch for the 1-inch curvature continues to improve with length. The patch will carry the majority of a tension load, therefore, the stresses in the patch due to a tension load on the plate needs to be considered as a design constraint.

E. CONVEX PLATE

The entire set of data for the convex plate geometry can be found in Figures 77 - 96 in the Appendix. Only the plots showing the worst case patch performance are included in the body of the thesis.

1. Convex Plate Change in Radius

When a convex plate is subjected to a tension load, the plate will tend to deflect away from the patch. Essentially making the crack at the adhesive interface act as a fulcrum and helping to open the crack at the free surface. Figure 32 shows the influence of this action as the depth of curvature is increased.

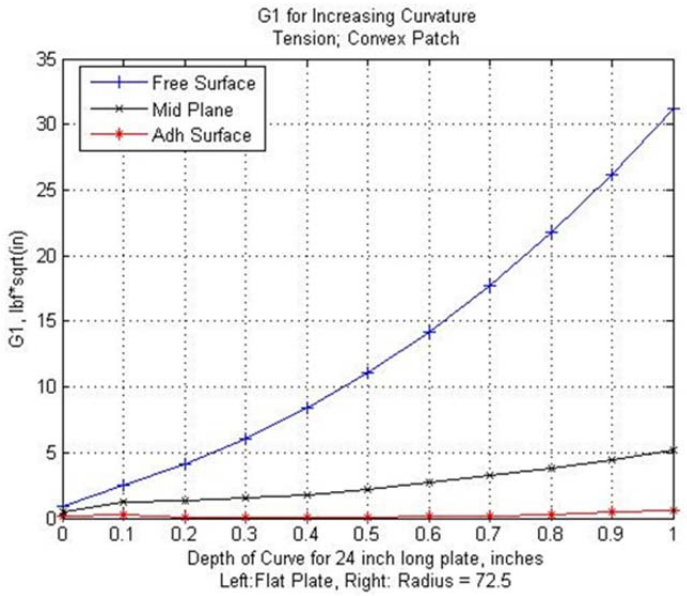

Figure 32. Change in radius, convex plate under tension

Analyzing the effect of curvature for a bending load produced some complex results. For constrained bending, the left side of Figure 33, the free surface is not visible because its plot is on the X-axis. Essentially, the load pushes the plate into the patch, closing the crack on the free surface. However, the free bending case produced an entirely different set of results and can be explained by the effect of the patch not fully extending through the width of the plate. Figure 34 is a contour plot generated by ANSYS highlighting the out of plane displacement of a convex plate with a depth of curvature of 0.9 inches. The darker color indicates a larger deflection. When subjected to a bending load on the unpatched side, the plate will bow in and increase the curvature. But since the patch does not extend all the way to the free edge, the portion of the plate not reinforced by the patch will deflect more in the out of plane deflection. The edge of the patch will create a fulcrum effect, pushing the free surface of the patched area outward. But the center of the crack does not deflect as much due to the crack, thereby causing a higher value of G1 at the free surface seen in the left side of Figure 33.

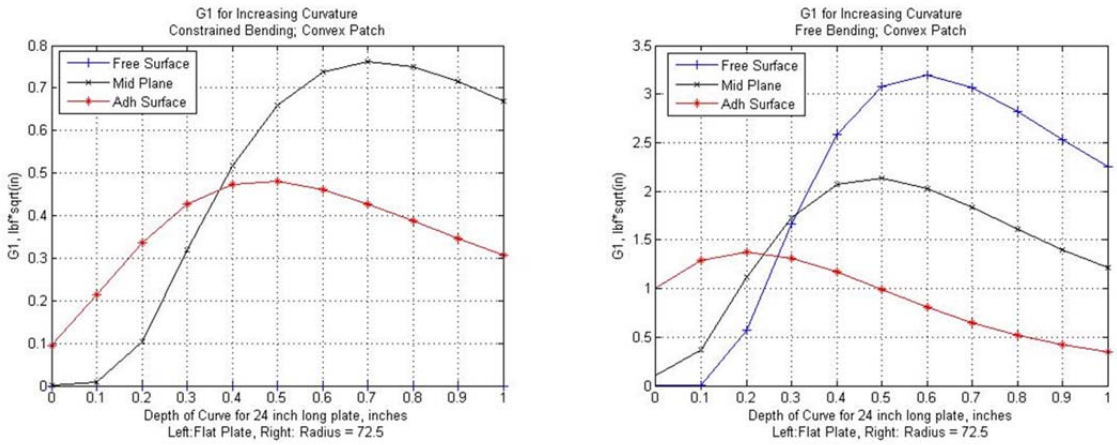

Figure 33. Change in radius, convex patch: L = constrained bending, R = Free bending

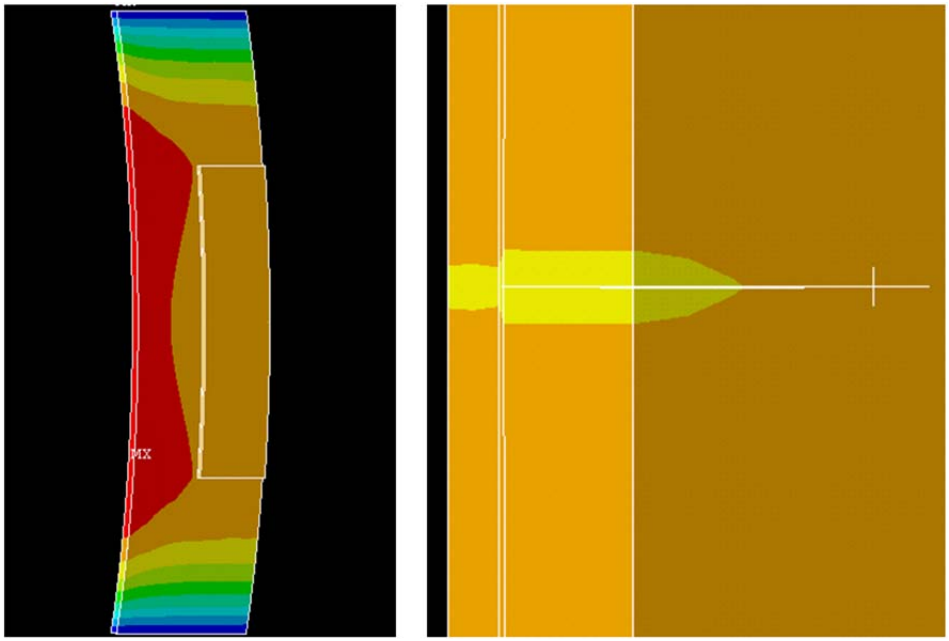

Figure 34. Out of plane deflection of a convex plate under free bending

2. Convex Plate, Half-Inch Depth of Curvature

a. Tension

The constant SR and varied dimensional parameter tests showing the worst case results can be found in Figures 35 and 36. Figure 35 shows that the system is in a fairly large state of bending, which tends more to tension for the smaller crack size. Also, Figures 35 and 36 both show that a smaller patch size has the better performance.

The dimension to be minimized is the patch length as seen in Figure 36, as the width had little effect on patch performance. Referring back to Figure 3, if the plates are being pulled in tension, then the patch edges along the length are acting as fulcrums to pull the center of the plate outward. Therefore, minimizing the patch length will minimize this effect and increase the effectiveness of the patch.

Although not tested as part of this thesis, it could be a reasonable assumption that tapering the edges of the patch will allow the plate to gradually deform the ends of the patch, thereby reducing bending imparted on the plate.

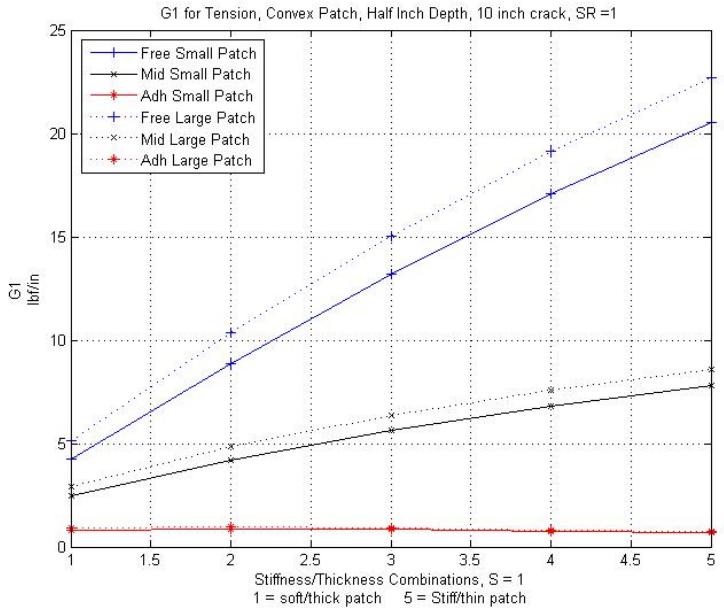

Figure 35. Constant SR, convex plate, tension, 10-inch crack

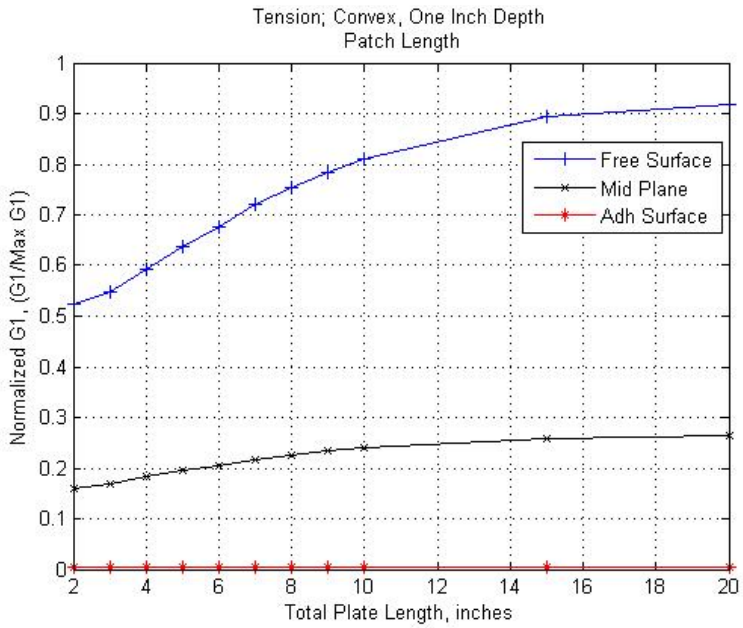

Figure 36. Convex plate, tension, 0.5-inch depth, vary patch length

b. Bending

The constant SR and varied dimensional parameter tests showing the worst case results for the free bending case can be found in Figures 37 and 38. The nearly horizontal lines in Figure 37 show that the system is close to being in pure tension and the same is true for the smaller crack size and for the constrained bending case. The constrained bending case also decreases the magnitude of G1 by a factor of about ten.

Figures 37 and 38 both show that a larger patch is a better design for the bending load case. Maximizing length has a significant improvement on patch performance. This is contrary to the results of the tension load case. Increasing the width of the patch also shows a potential increase in performance of as much as 10%. The maximum performance is reached when the patch width extends to about 75% of the total plate width.

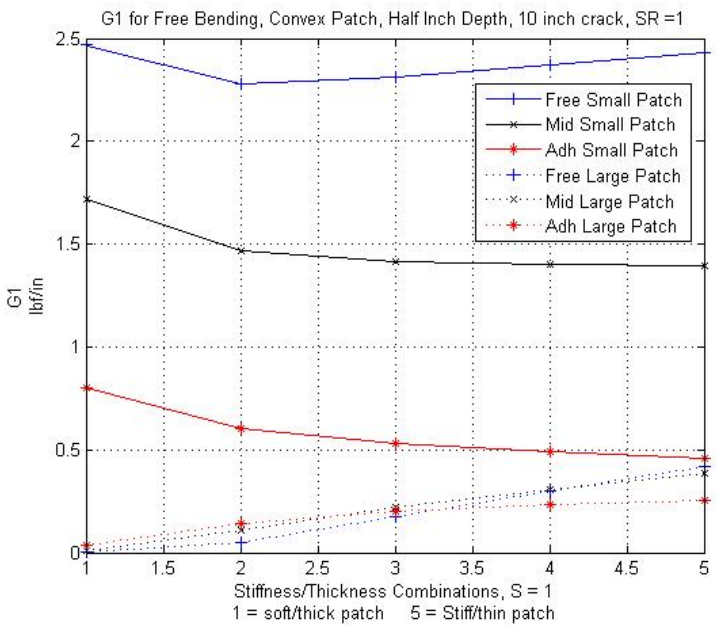

Figure 37. Constant SR, convex plate, free bending, 0.5-inch depth, 10-inch crack

The requirements for patch length on a 0.5-inch depth convex plate are opposite than those for optimal performance for a tension and bending load applied to the host plate. A more detailed analysis is required, and although not a part of this thesis, it is suggested that a possible solution would be an optimal ply drop-off sequence. However, if the plate is not expected to have a bending load applied, such as a vertical plate not subjected to wave loading, then the patch should be optimized for the tension case.

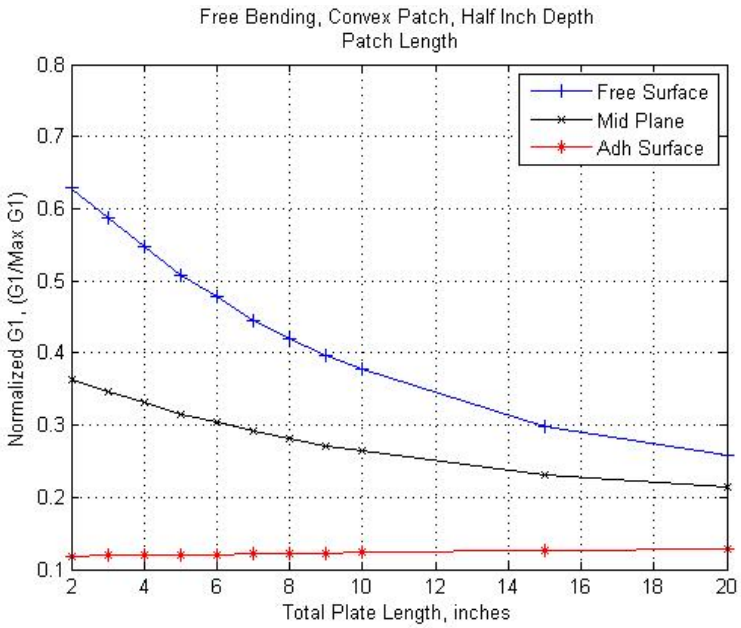

Figure 38. Convex plate, free bending, 0.5-inch depth, vary patch length

3. Convex Plate, 1-Inch Depth of Curvature

a. Tension

The constant SR and varied dimensional parameter tests showing the worst case results for the tension case on a 1-inch depth curved plate can be found in Figures 39 and 40. The same conclusions for the 0.5-inch depth plate can be made for the 1-inch depth plate. The only significant difference between the two geometries is the magnitude of G1. As the curve of the plate increases, G1 also increases.

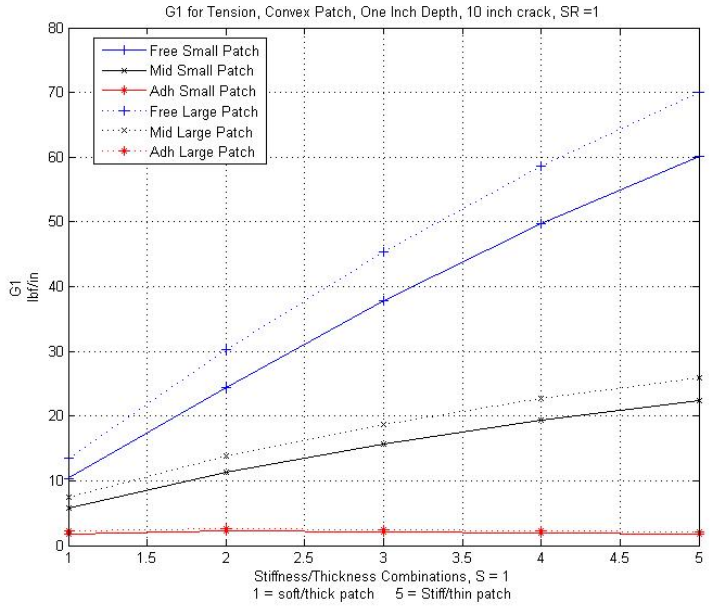

Figure 39. Constant SR, convex plate, tension, 10-inch crack

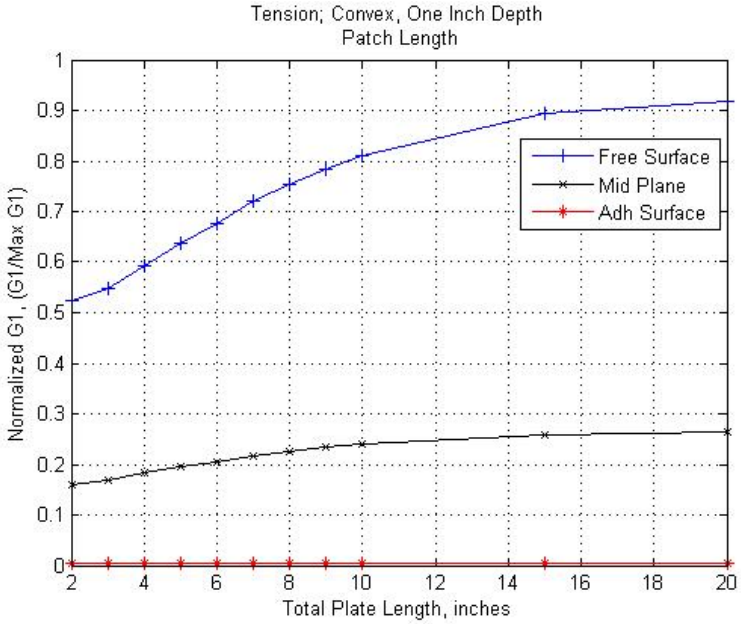

Figure 40. Convex plate, tension, 1-inch depth, vary patch length

b. Bending

The same conclusions from the constant SR test can be made for the 1-inch depth as were made for the 0.5-inch depth. As seen in Figure 41, the system is generally in a state of tension and a larger patch is better.

The varied dimensional parameter set of tests indicate some important differences for the more curved plate. As seen in the Figure 42, the varied patch length test for free bending conditions, a patch that is too short may make the crack grow faster than if it was left unpatched. For the constrained bending case, a reduction in G1 of 40 – nearly 80% can be achieved. The difference between the free bending and constrained bending case show the significance of a clamped edge on crack growth. Increasing the width of the patch will also increase effectiveness of the patch. Extending the patch width can achieve a 10% increase in patch effectiveness. The optimum width is reached and then plateaus at a patch width of about ½ the plate width for constrained bending and about ¾ plate width for the free bending case.

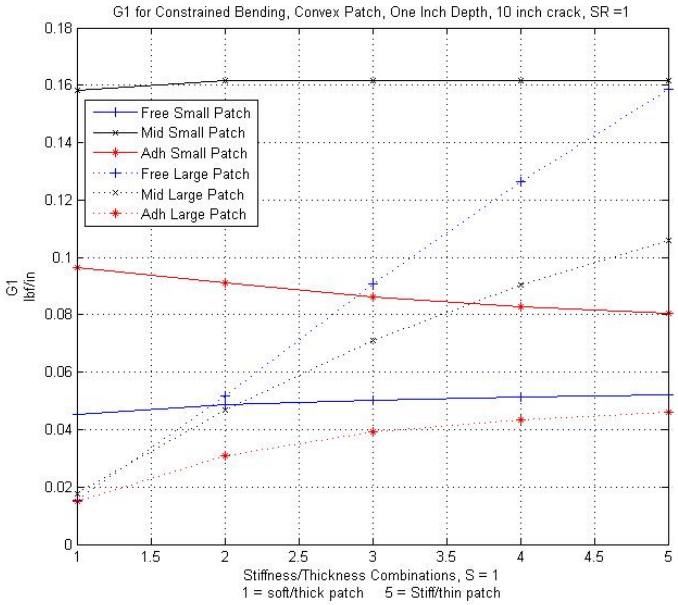

Figure 41. Constant SR, convex plate, bending, 10-inch crack

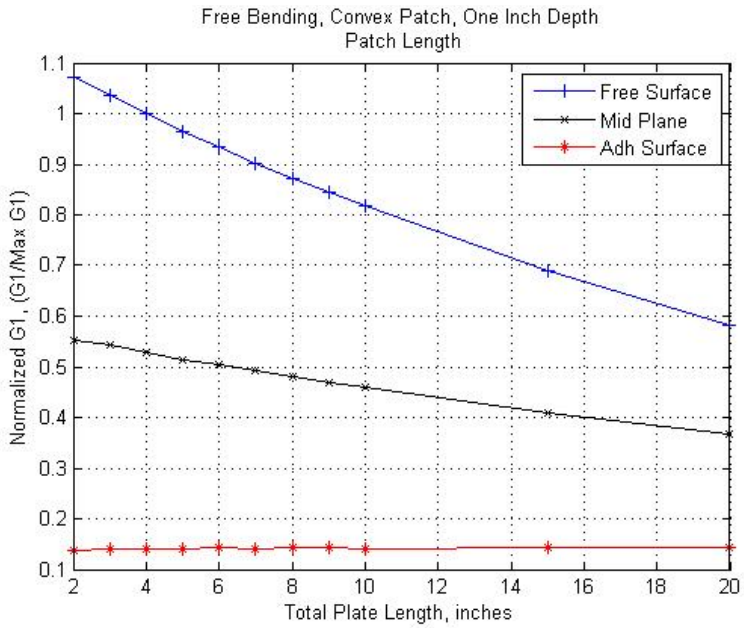

Figure 42. Convex plate, free bending, 1-inch depth, vary patch length

c. Convex Plate Summary

For a convex plate, the optimum patch size is opposite depending on the expected load case. For a load case of tension applied to the base plate, a smaller patch is more effective whereas for a bending load, a larger patch is more effective. Careful consideration is needed in determining which load case is more important. The depth of curvature and proximity of the crack to a clamped edge are significant points. For example, the presence of a patch that is too short on a plate with a crack far from the welded joint could result in an overall increase in the rate at which the crack would grow. For situations where there is not a clear dominant load case, it is suggested that a ply drop-off sequence may help mitigate the negative effect of length for a tensile load.

THIS PAGE INTENTIONALLY LEFT BLANK

IV. CONCLUSIONS AND RECOMMENDATIONS

A. CONCLUSIONS

The effect of the different loading conditions, boundary conditions, panel geometries and patch location relative to the applied load have a significant impact on the effectiveness of a cracked panel repaired with a bonded composite patch. Even the small changes in curvature that could occur due to warping or other issues from aging are worth considering.

1. Modeling

When modeling a cracked plate repaired with a bonded patch, non-linear geometric analysis is required for all cases, even if the deflection is very small. In addition, there are bending cases where the crack faces could come in contact. For those cases, the crack face must be modeled using contact elements. The inclusion of an adhesive layer in the model is required. Once included, the thickness of the adhesive layer had a minor effect and is recommended to use a slightly thicker layer in the model to reduce the poor element aspect ratios.

2. General Effects of Curvature

The curvature of a plate has the largest negative impact on G1 when the plate is only slightly curved. In that condition, the curvature of the plate creates a bending stress that increases G1. Once the curvature of the plate increases to a certain, G1 will begin to decrease and become more uniform through the thickness of the plate.

3. Flat Plate

For a flat plate, the critical load case is tension. Bending with the load applied to the patched side should also be considered if that is where the patch has to be placed. Applying the patch on the opposite side of the expected bending load will result in the load being almost completely transferred to the patch. If accessibility to the repair area allows, applying a patch opposite of the expected bending load is the best configuration.

The patch can be designed to minimize G1 for the expected tensile loading and the ability of the patch to withstand the expected bending load becomes a design constraint.

4. Concave Plate

For a concave plate, the least critical load condition in terms of G1 is tension. If the plate is subjected to a tensile load, the patch will carry the majority of the load.

Bending is the critical loading condition for this geometry. Increasing both the length and width of the patch improve the performance, with the patch length offering the larger increase in performance. The performance of the patch either plateaus or continues to improve with patch size so it is recommended to maximize the size of the patch in both length and width.

5. Convex Plate

For a convex plate, both tension and bending are relevant load cases. And the optimization for one load case is counter to optimization of the other. By examining the geometry of a convex patched plate, it is suggested that the negative effect off patch length on G1 can be mitigated through the use of ply drop-offs which will gradually soften the edges of the patch. However, careful consideration should be given to the location of the crack relative to a clamped boundary as well as the curvature of the plate. A plate with a poorly designed patch applied to the convex side could result in an increased rate of crack growth.

B. RECOMMENDATIONS

1. Regarding the Application of Composite Patches

Increasing the thickness or using a stronger material will improve the performance of a composite patch. To the best of the author's knowledge, the current standard material used for applications on naval ships is E-glass [1]. Considering the cost, availability, ease of use, there is nothing in this thesis that would indicate the need to change material. The use of E-glass with an appropriate thickness was able to effect a reduction in G1 to some useful extent for each plate and load case analyzed.

Previous work outlined in the literature showed a significant improvement for a double-sided patch. Accessibility restrictions to the repair area make this difficult on a Navy ship. However, the double-side patch is recommended whenever the situation allows. In most cases considered, the effectiveness of a patch was influenced greatly by the side of the plate relative to the plate curvature or to an applied bending load in which the patch was placed. For a flat plate with a patch applied to the side opposite of the expected bending load and a concave plate subjected to a tension load, it was found that the patch will carry the majority of the load. In these two cases, the optimization in reducing G1 should be shifted to the other load case. The case in which the patch will carry close to the entire load should be used to define design constraints.

2. Future Work

a. Investigate and Determine Alternate Stiffness Ratios

The idea for a different stiffness ratio was suggested in the testing overview section of this thesis. In addition a simple technique to determine a value of n using finite element analysis was introduced. The basic hypothesis is any single-sided patched system will have some level of bending induced by the asymmetric geometry, and therefore a ratio that represents a true stiffness match between the plate and the patch is Equation 7 where n will lie between 1 and 3. Using this stiffness ratio will better optimize the reduction of G1 and could help to reduce the stress attraction effect. A thorough investigation is suggested to determine the optimal value of n for each type of system, and how sensitive it is to the various parameters such as curvature, loading and patch dimension.

b. Conduct Full System Analysis for Systems Designated as Design Constraints

Two conditions were identified as design constraints. It was determined that a bending load applied to the opposite side of a patch on a flat plate and a tensile load applied to a concave plate would result in the patch carrying the majority of load. These

conditions should be used to establish design constraints on the patch. However, in order to establish these constraints, the loading condition on the patched systems needs to be fully understood.

c. Conduct a Full Thermal Stress Analysis for Patched Clamped Plates

To the best of the author's knowledge, previous work on thermal residual stresses in bonded composite repairs assumed an infinite plate model. This assumption may not apply to shipboard systems. A panel will deflect outwards or inwards when heated due to thermal expansion due to the edges being welded to the support structure. Therefore during the curing process, the base plate is deflected and in a state of compression. The patch, however, is free to move and not in any state of stress. Once cured, the plate will want to return to its normal position and the patch will resist. The plate will be in a state of compression and the post-curing reduction in temperature might work to close the crack more. Understanding the residual thermal stresses might show that maximizing the curing temperature within the acceptable range of the adhesive could be used as an additional parameter to increase patch effectiveness.

APPENDIX: DATA PLOTS

A. PLATE ONLY IMAGES

1. Change in Radius Test

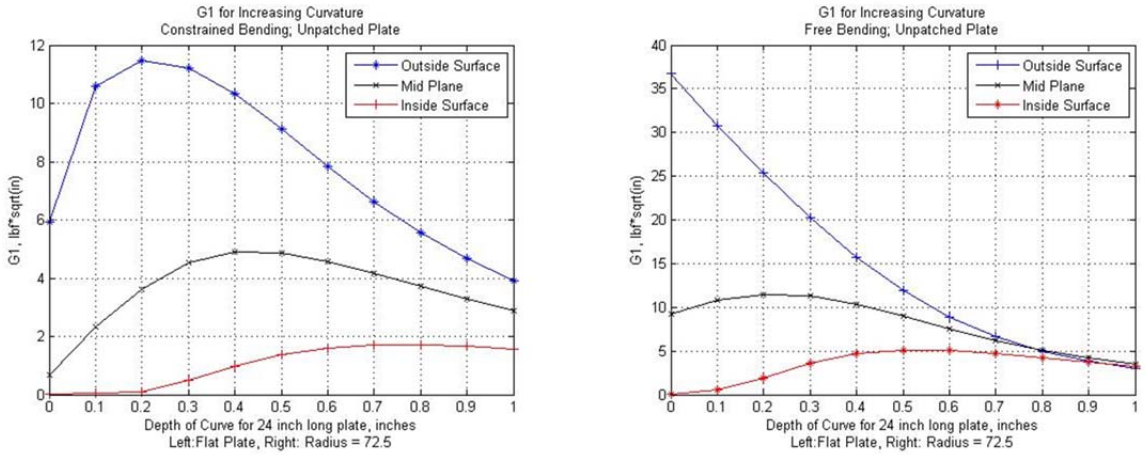

Figure 43. Unpatched plate change in radius

B. FLAT PLATE IMAGES

1. Varied Dimensional Parameters

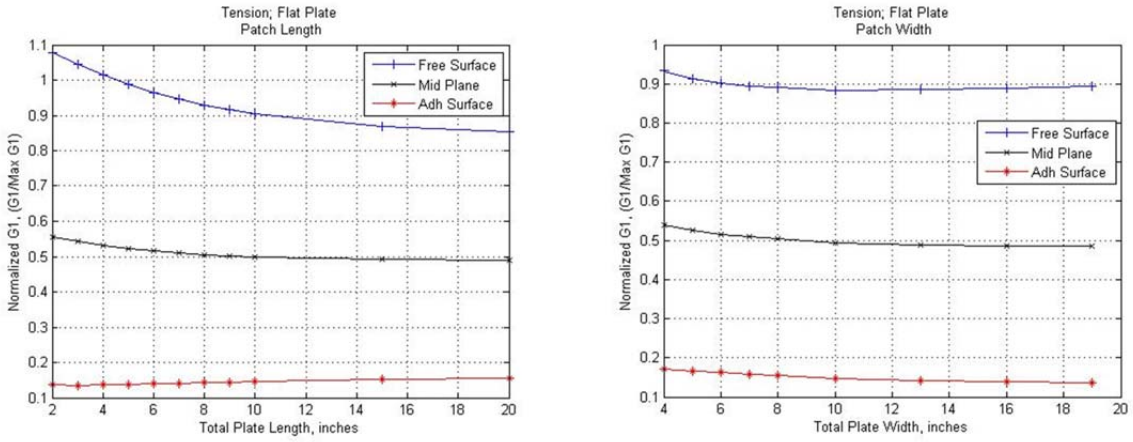

Figure 44. Flat plate, tension, Left = vary length, Right = vary width

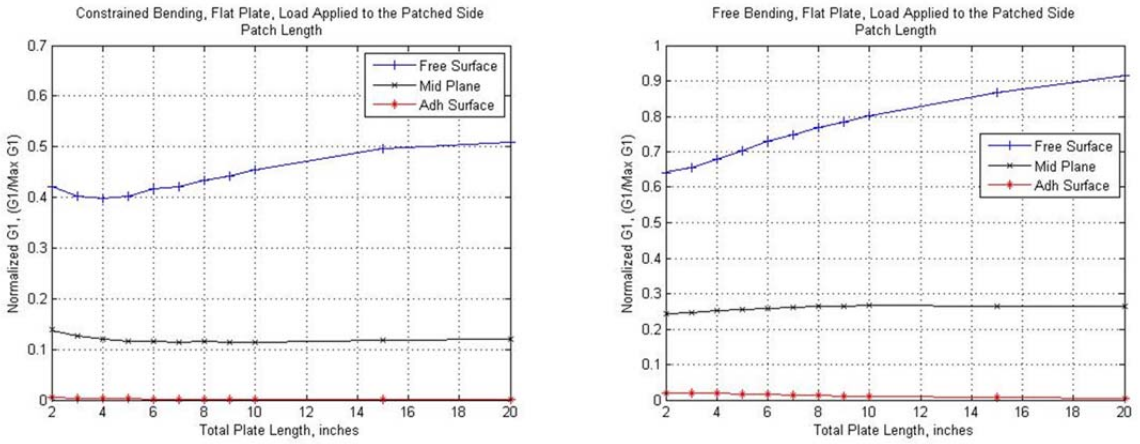

Figure 45. Flat plate bending, vary length, patch side loading, Left = constrained bending, Right = free bending

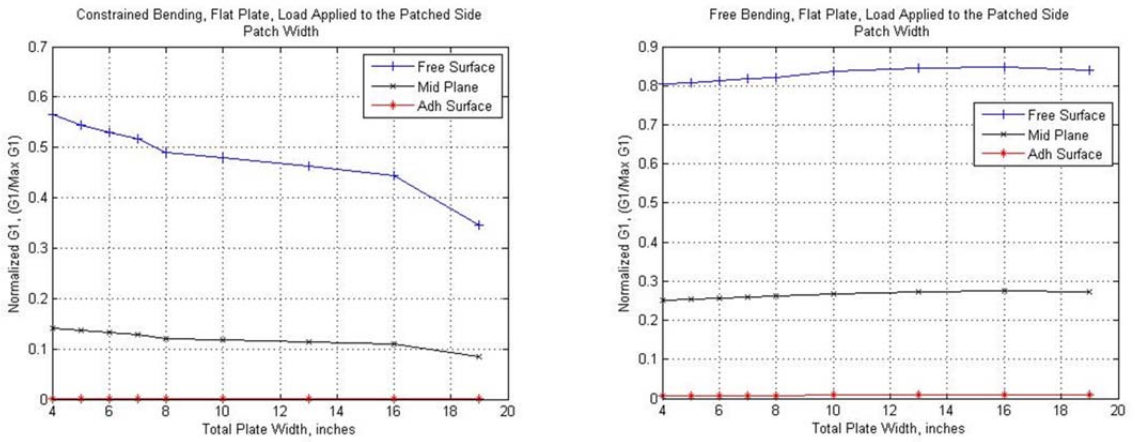

Figure 46. Flat plate bending, vary width, patch side loading, Left = constrained bending, Right = free bending

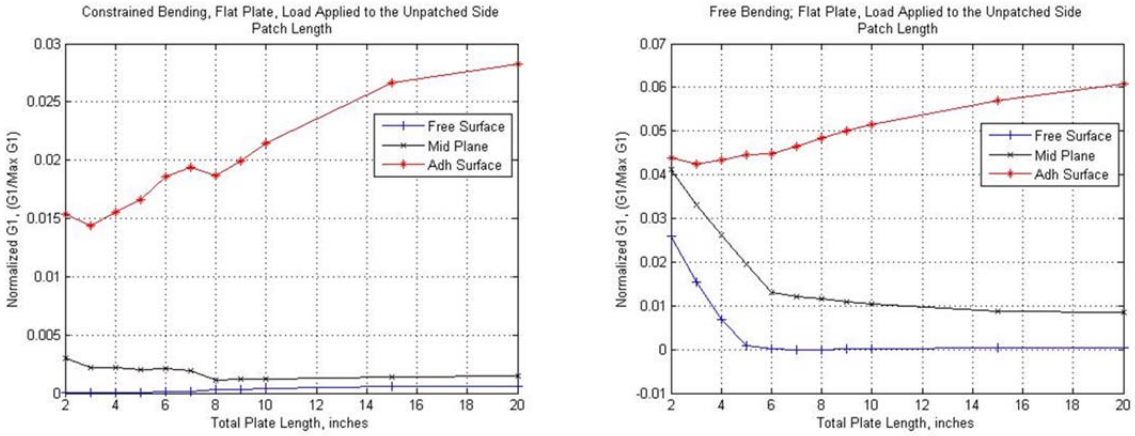

Figure 47. Flat plate bending, vary length, unpatched side loading, Left = constrained bending, Right = free bending

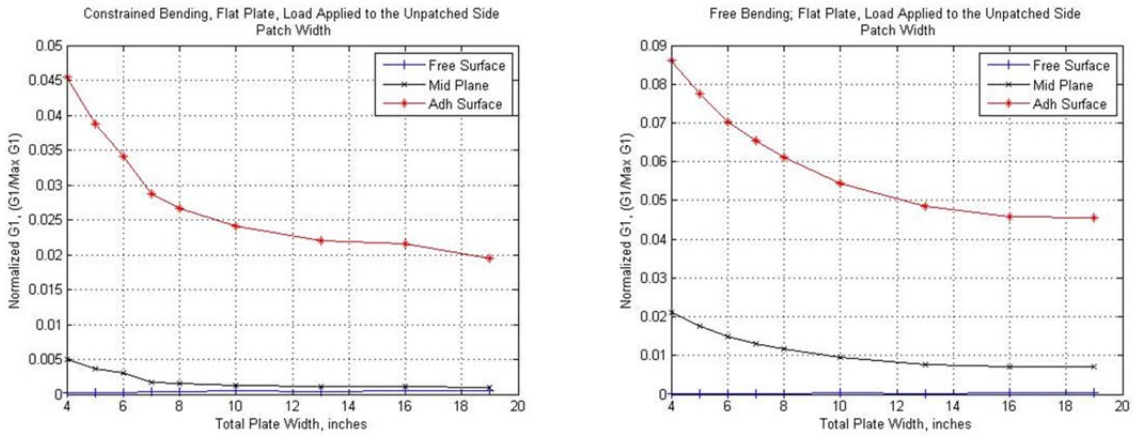

Figure 48. Flat plate bending, vary width, patch side loading, Left = constrained bending, Right = free bending

2. Constant Stiffness Ratio

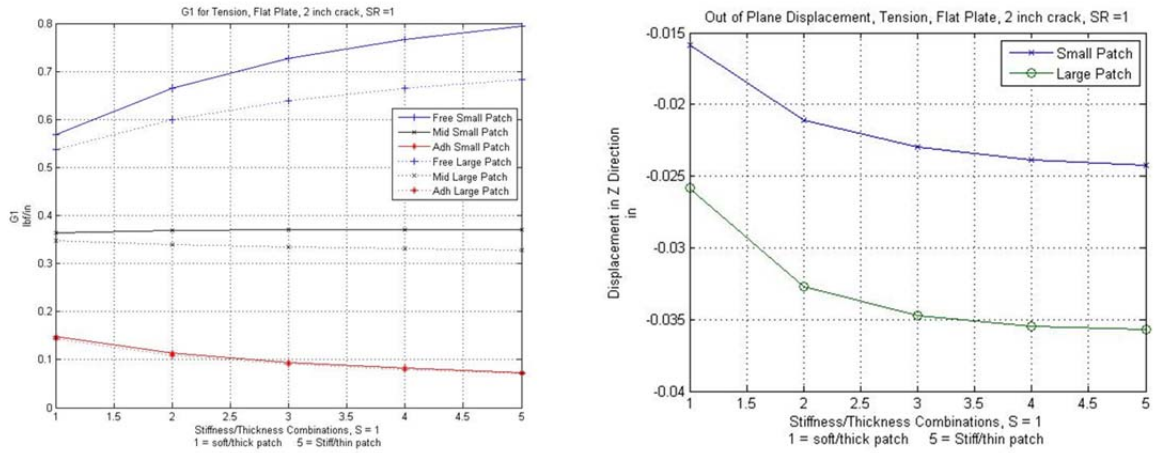

Figure 49. SR, tension, flat plate 2-in. crack, Left = G1, Right = out of plane displacement

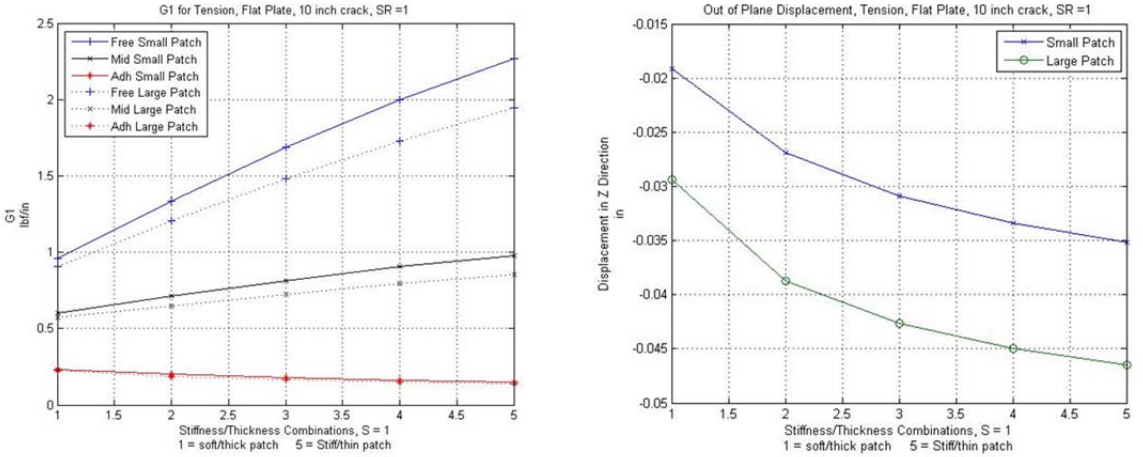

Figure 50. SR, tension, flat plate 10-in. crack, Left = G1, Right = out of plane displacement

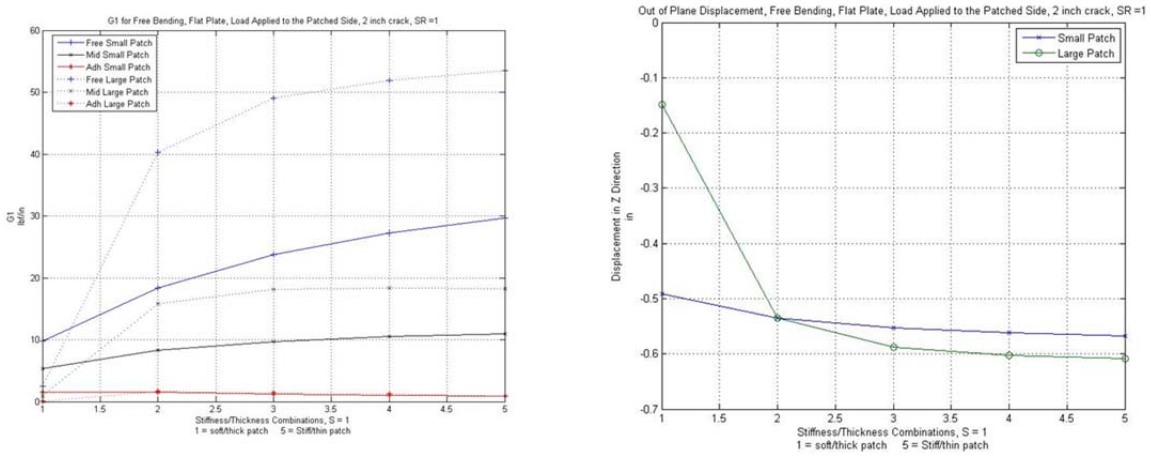

Figure 51. SR, free bending, unpatched side loading, flat plate 2-inch crack, Left = G1, Right = out of plane displacement

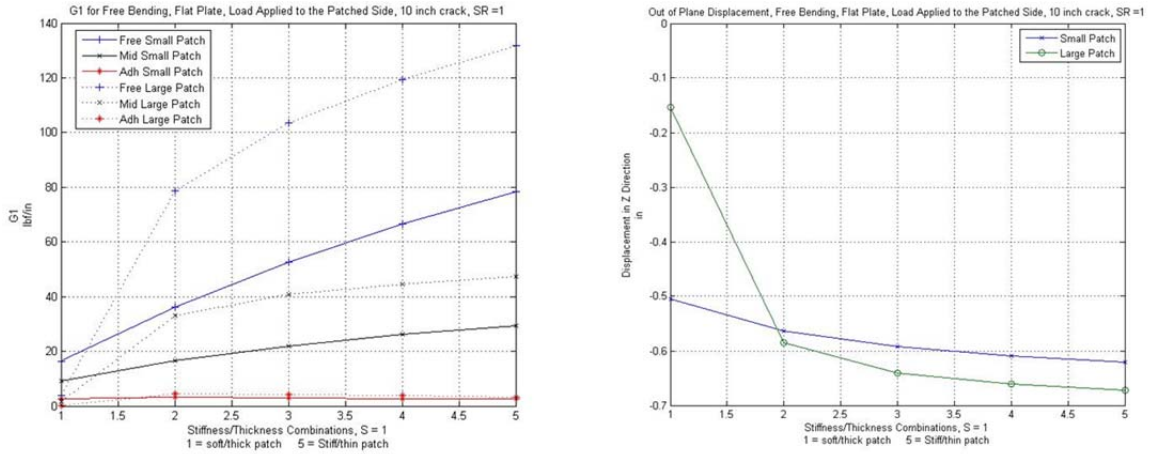

Figure 52. SR, free bending, unpatched side loading, flat plate 10-inch crack, Left = G1, Right = out of plane displacement

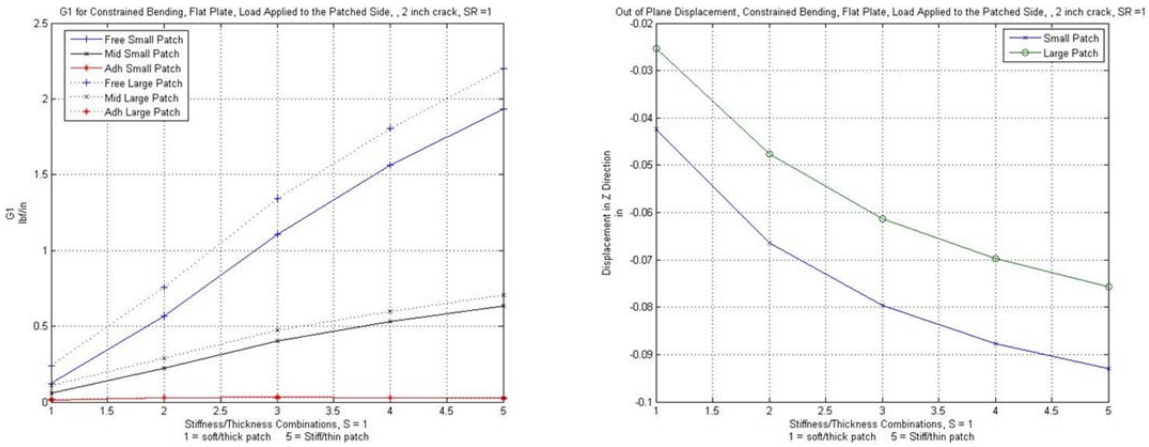

Figure 53. SR, constrained bending, patched side loading, flat plate 2-inch crack, Left = G1, Right = out of plane displacement

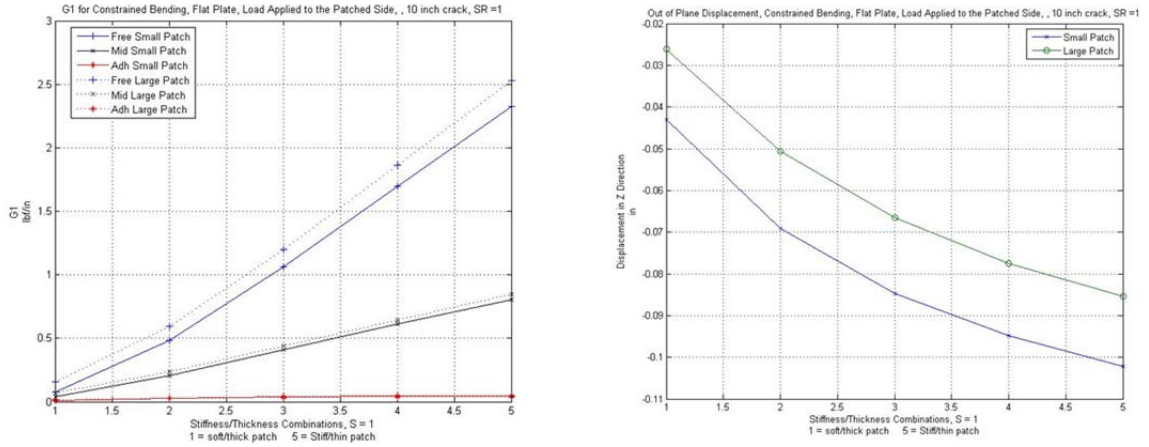

Figure 54. SR, constrained bending, patched side loading, flat plate 10-inch crack, Left = G1, Right = out of plane displacement

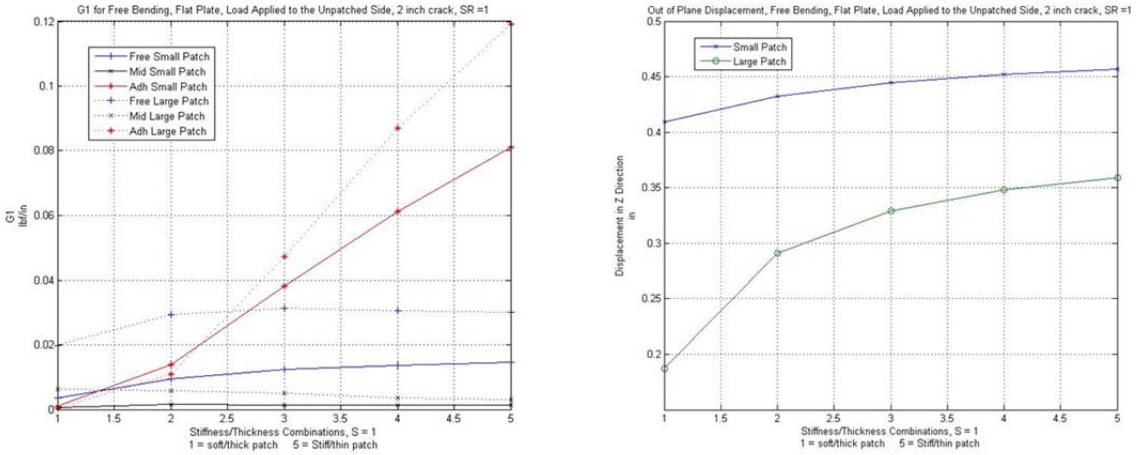

Figure 55. SR, free bending, unpatched side loading, flat Plate 2-inch crack, Left = G1, Right = out of plane displacement

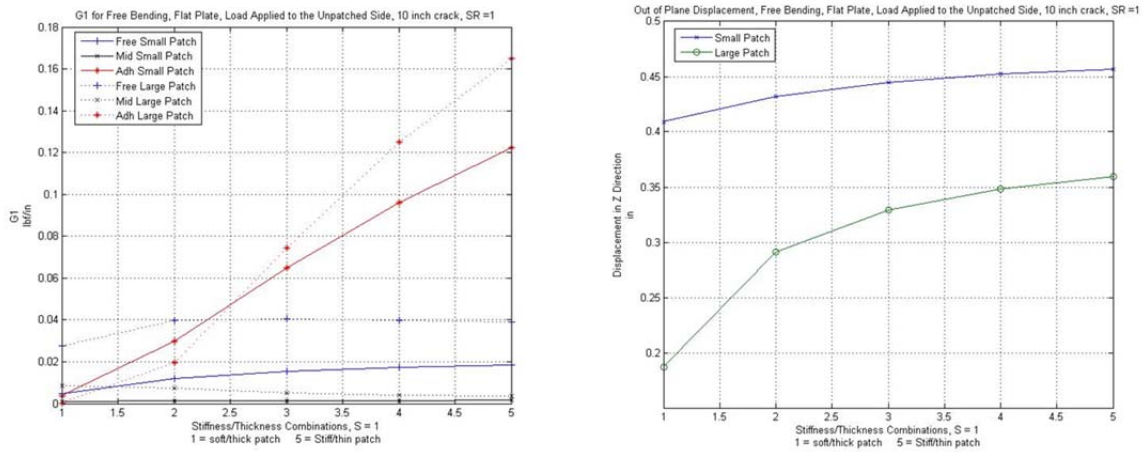

Figure 56. SR, free bending, unpatched side loading, flat plate 10-inch crack, Left = G1, Right = out of plane displacement

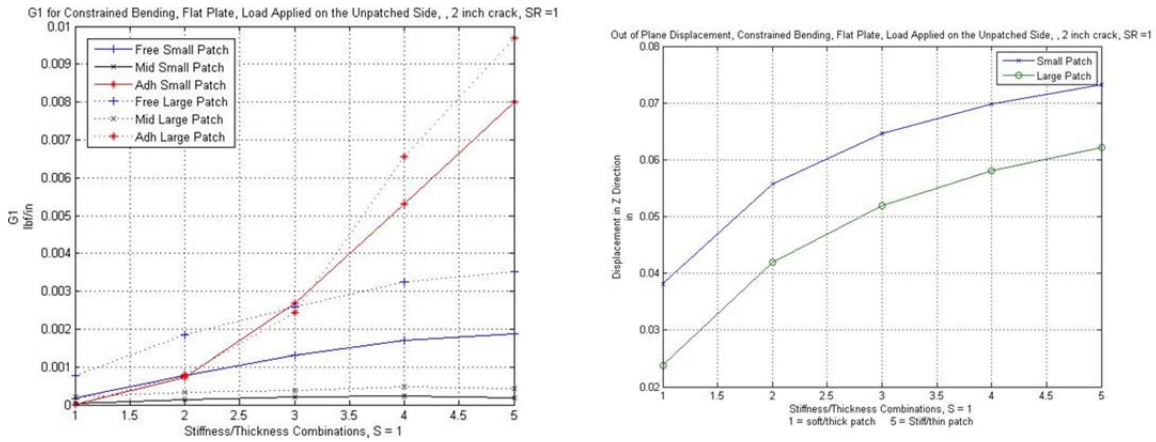

Figure 57. SR, constrained bending, unpatched side loading, flat plate 2-inch crack, Left = G1, Right = out of plane displacement

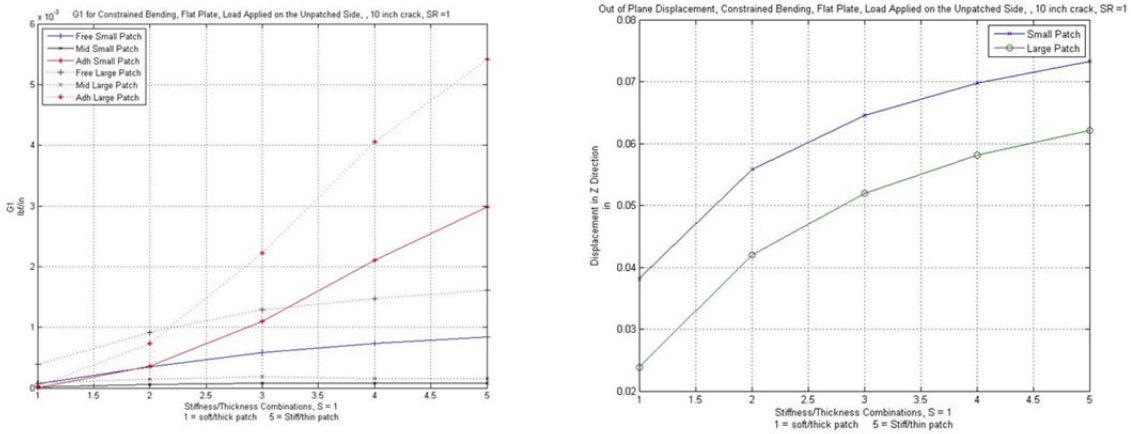

Figure 58. SR, constrained bending, unpatched side loading, flat plate 10-inch crack, Left = G1, Right = out of plane displacement

C. CONCAVE PLATE IMAGES

1. Change in Radius Test

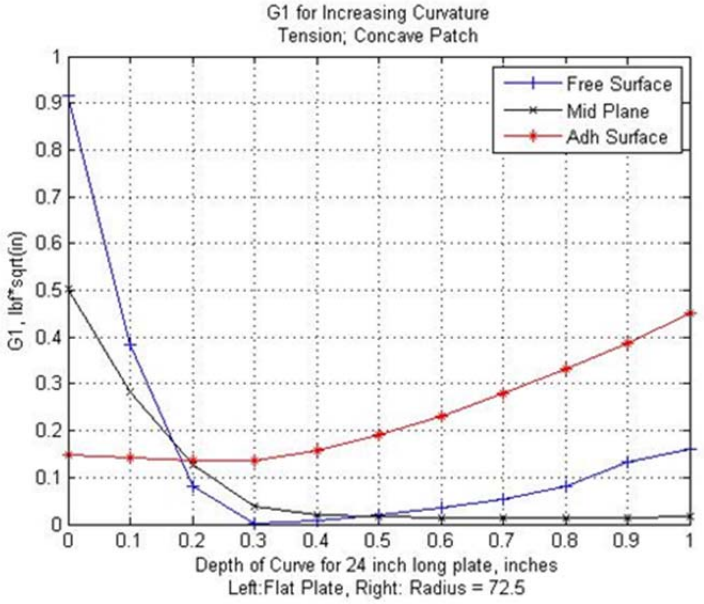

Figure 59. Change in radius, tension, concave plate

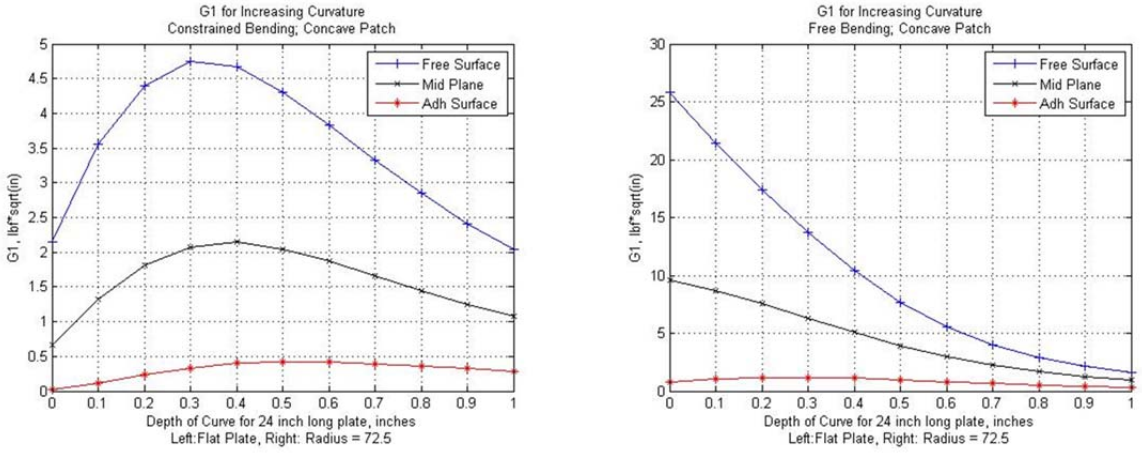

Figure 60. Change in radius, bending, concave plate

2. Varied Dimensional Parameters

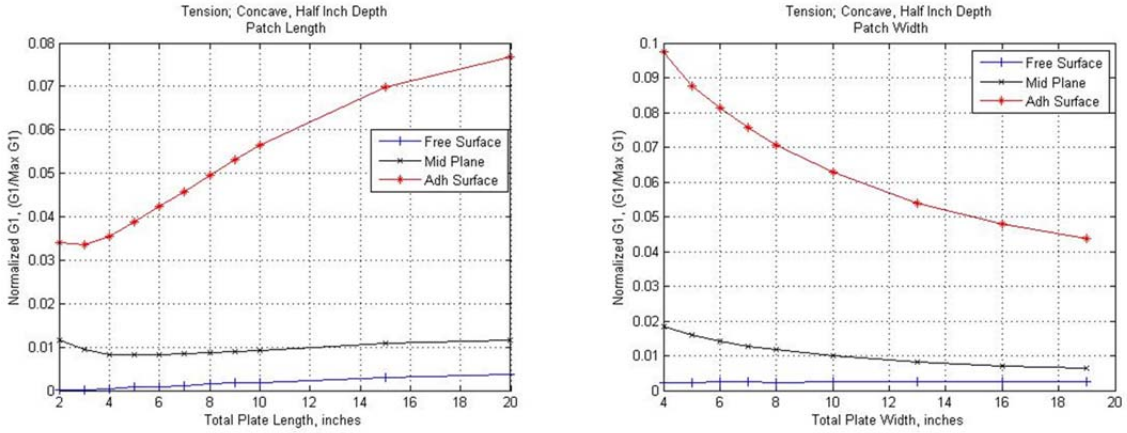

Figure 61. Concave, tension, 0.5-inch depth, Left = vary length, Right = vary width

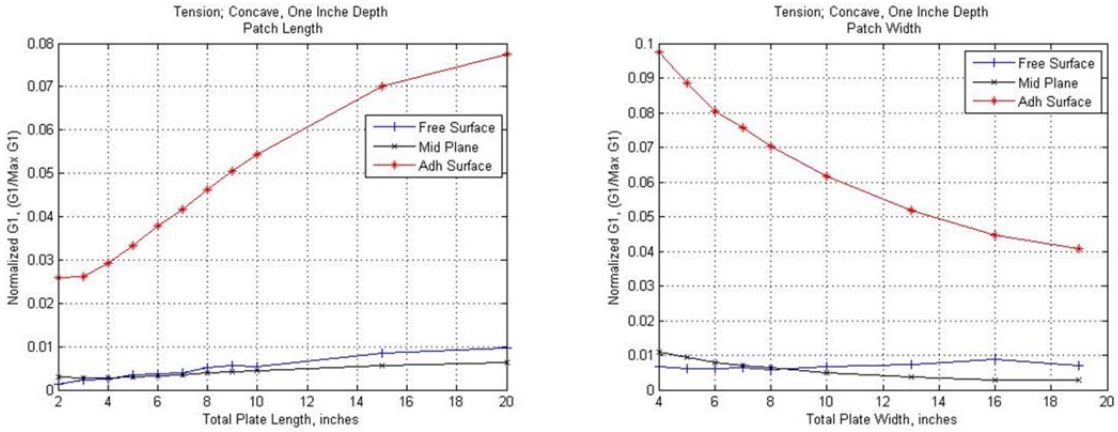

Figure 62. Concave, tension, 1-inch depth, Left = vary length, Right = vary width

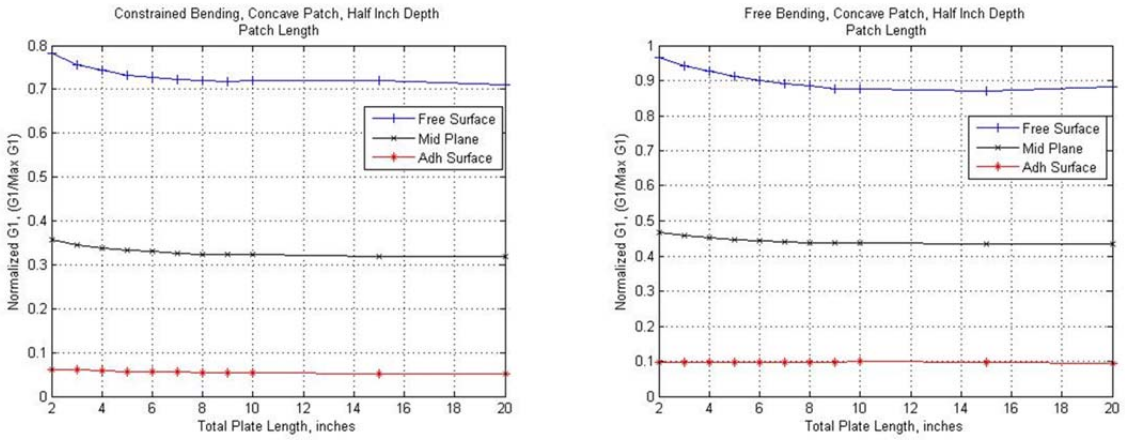

Figure 63. Concave, vary length, 0.5-inch depth, Left = constrained bending, Right = free bending

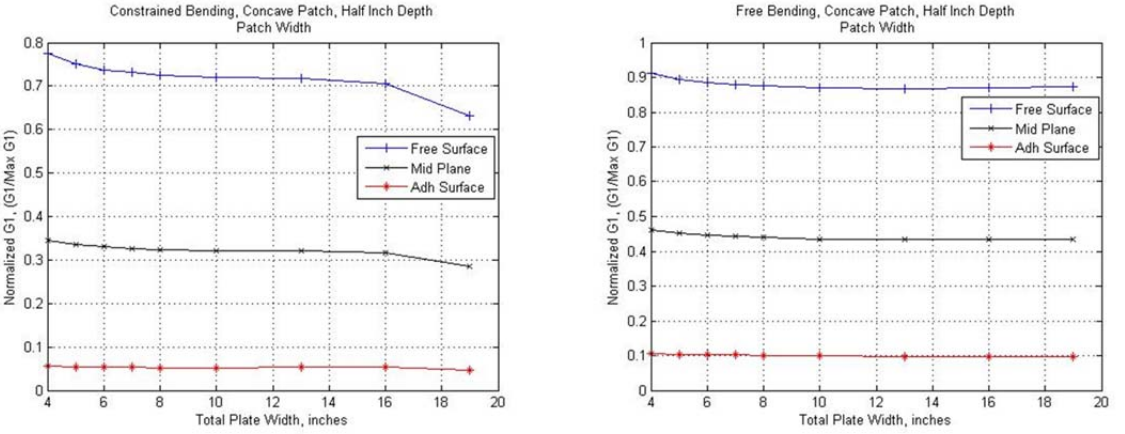

Figure 64. Concave, vary width, 0.5-inch depth, Left = constrained bending, Right = free bending

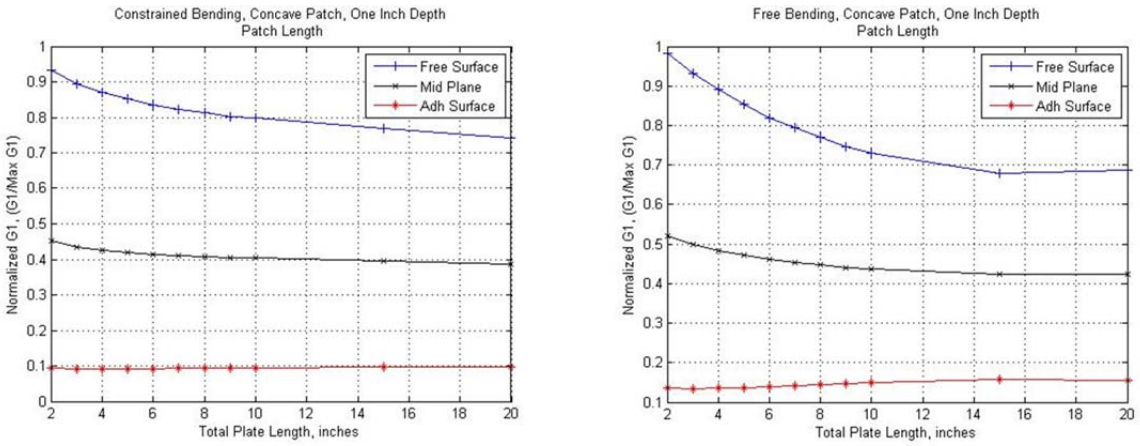

Figure 65. Concave, vary length, 1-inch depth, Left = constrained bending, Right = free bending

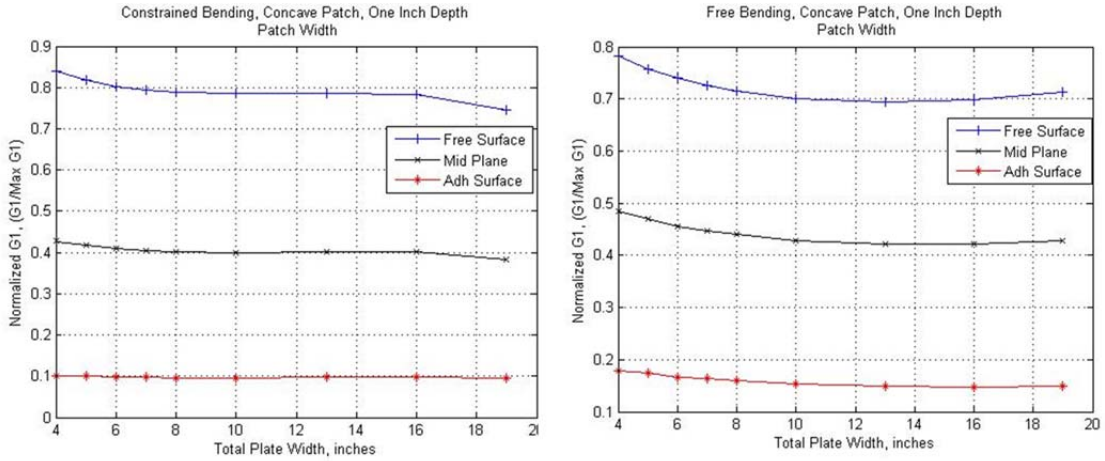

Figure 66. Concave, vary width, 1-inch depth, Left = constrained bending, Right = free bending

3. Constant Stiffness Ratio

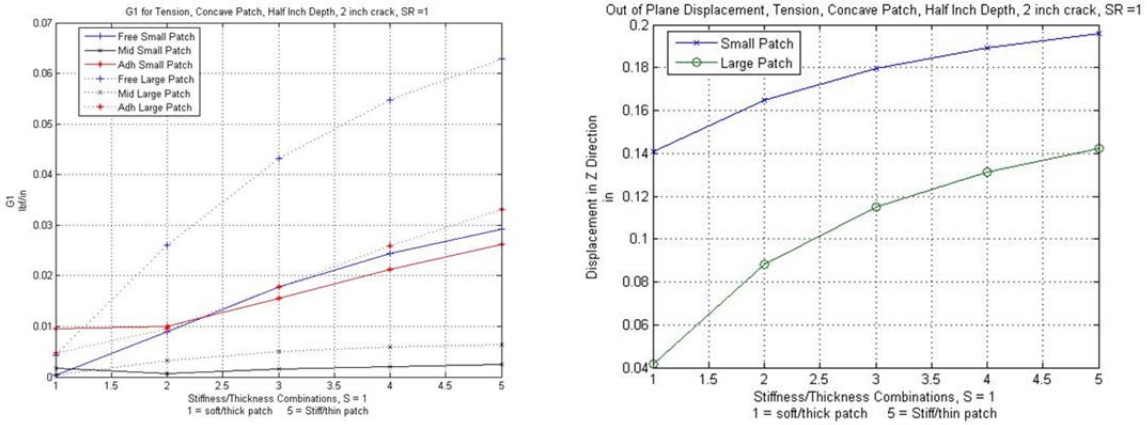

Figure 67. CS, tension, concave patch, 0.5-inch depth, 2-inch crack, Left = G1, Right = out of plane displacement

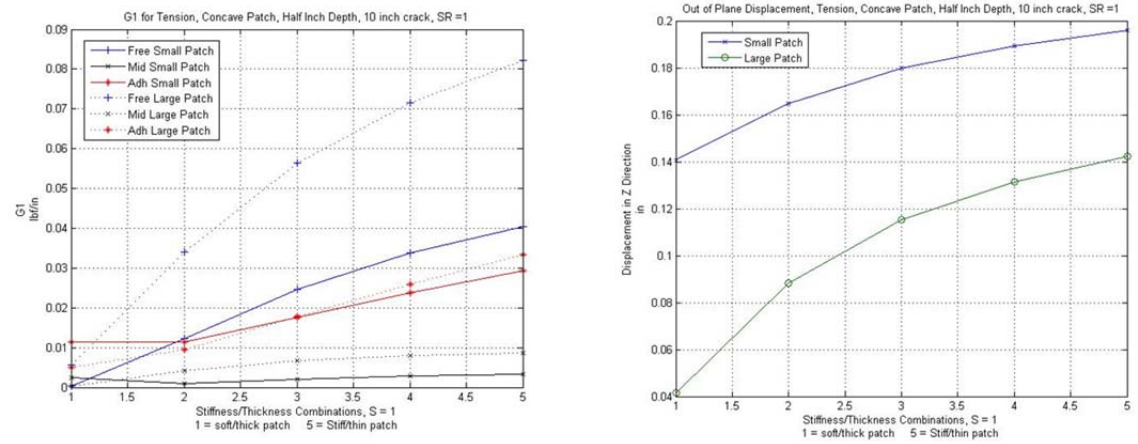

Figure 68. CS, tension, concave patch, 0.5-inch depth, 10-inch crack, Left = G1, Right = out of plane displacement

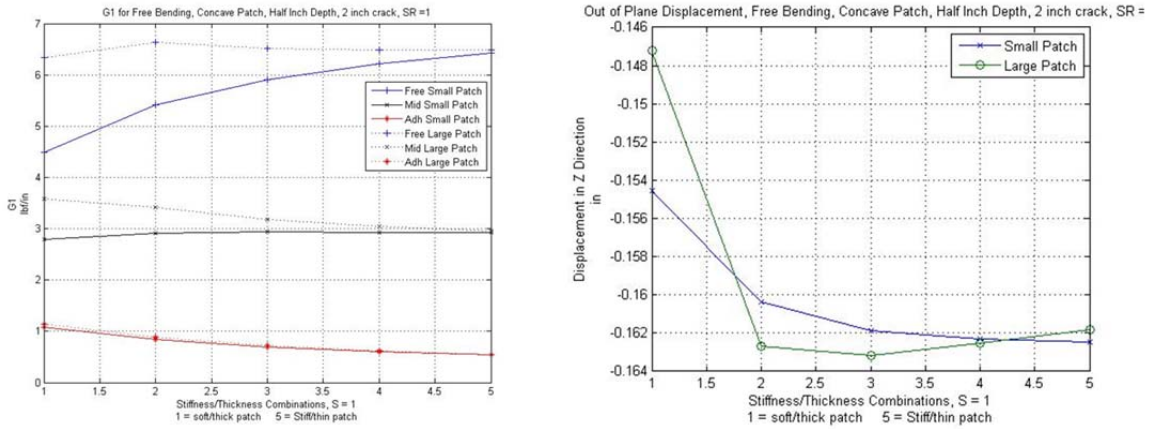

Figure 69. CS, free bending, concave patch, 0.5-inch depth, 2-inch crack, Left = G1, Right = out of plane displacement

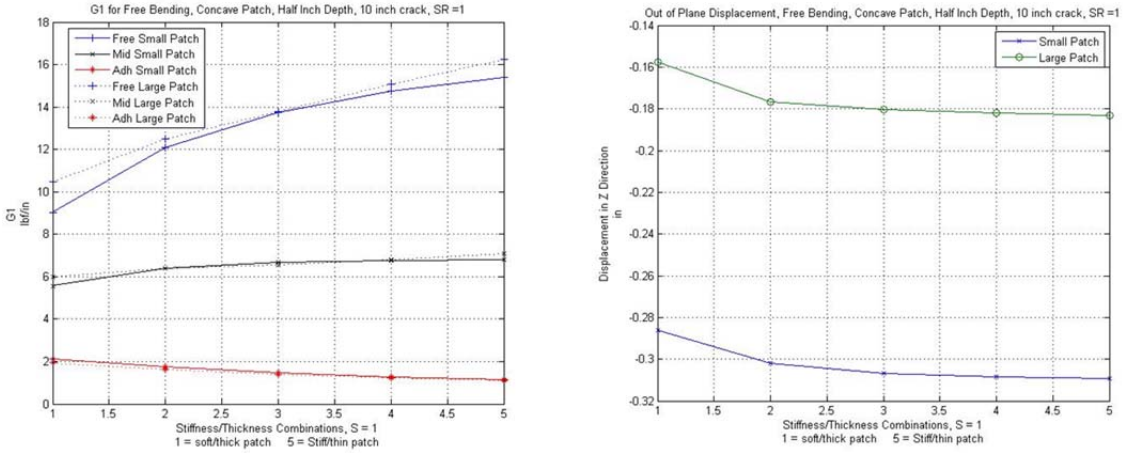

Figure 70. CS, free bending, concave patch, 0.5-inch depth, 10-inch crack, Left = G1, Right = out of plane displacement

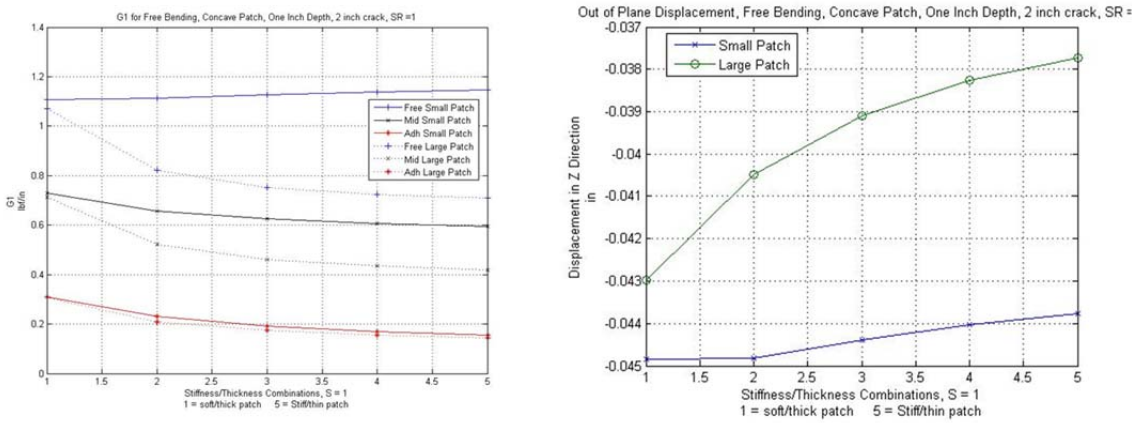

Figure 71. CS, free bending, concave patch, 1-inch depth, 2-inch crack, Left = G1, Right = out of plane displacement

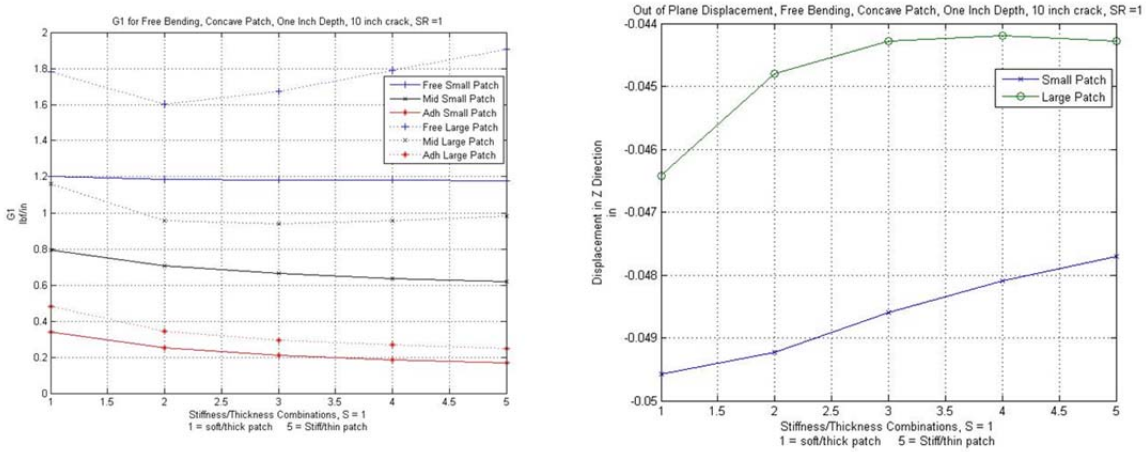

Figure 72. CS, free bending, concave patch, 1-inch depth, 10-inch crack, Left = G1, Right = out of plane displacement

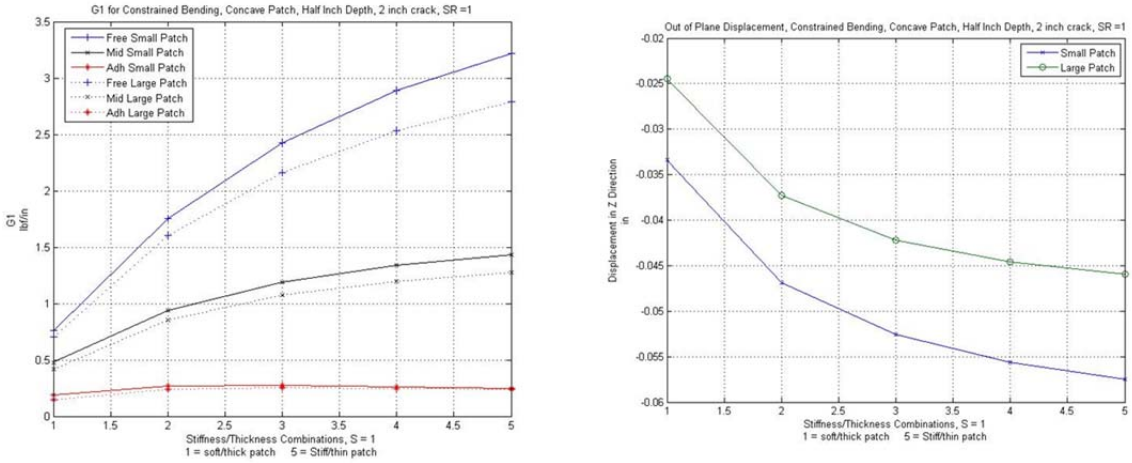

Figure 73. CS, free bending, concave patch, 0.5-inch depth, 2-inch crack, Left = G1, Right = out of plane displacement

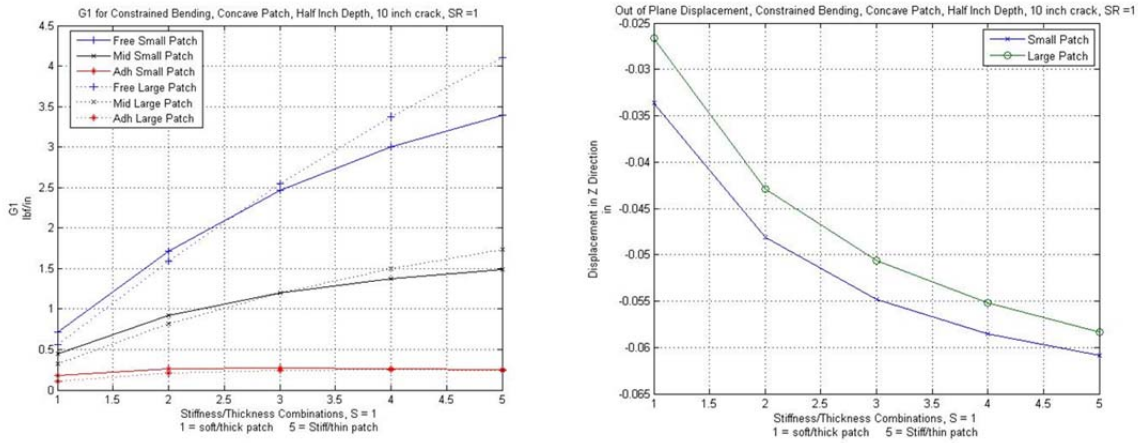

Figure 74. CS, constrained bending, concave patch, 0.5-inch depth, 10-inch crack, Left = G1, Right = out of plane displacement

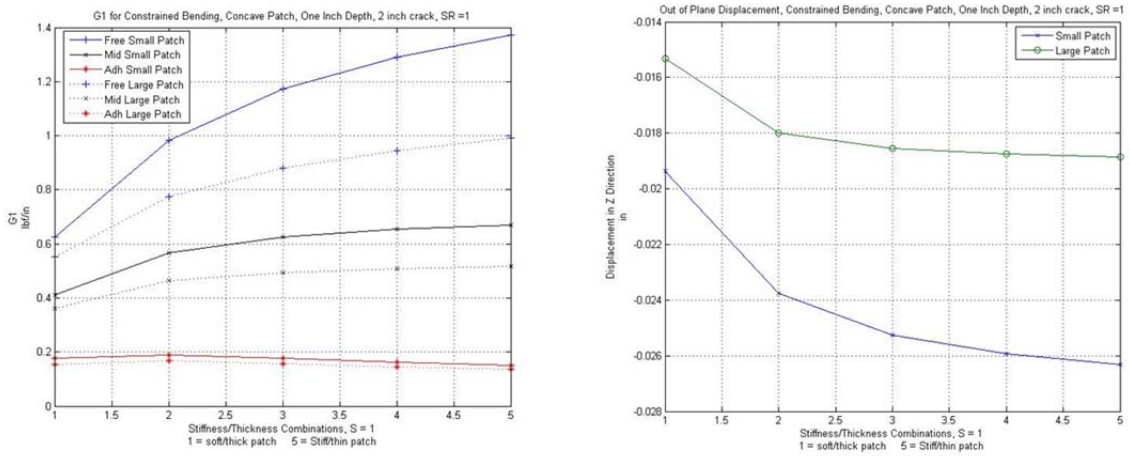

Figure 75. CS, constrained bending, concave patch, 1-inch depth, 2-inch crack, Left = G1, Right = out of plane displacement

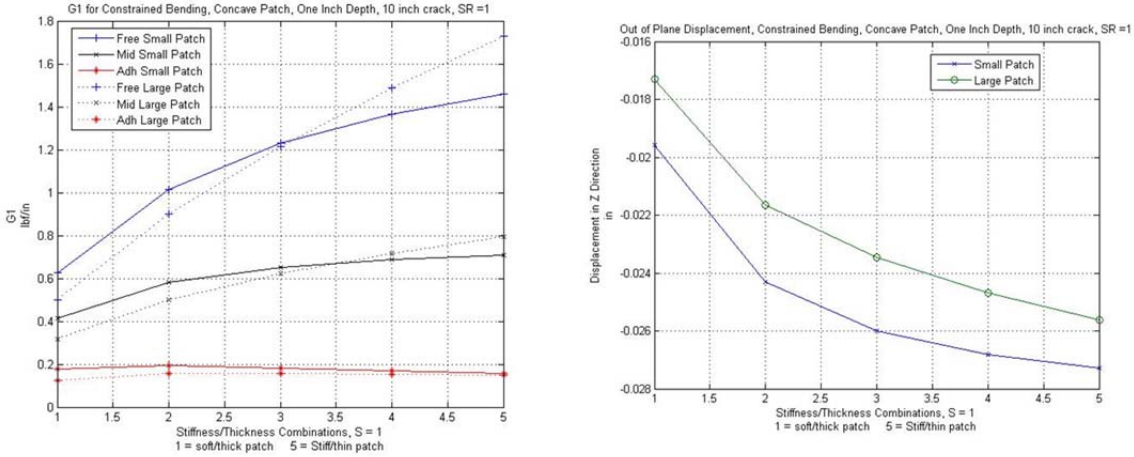

Figure 76. CS, constrained bending, concave patch, 1-inch depth, 10-inch crack, Left = G1, Right = out of plane displacement

D. CONVEX PLATE IMAGES

1. Varied Dimensional Parameters

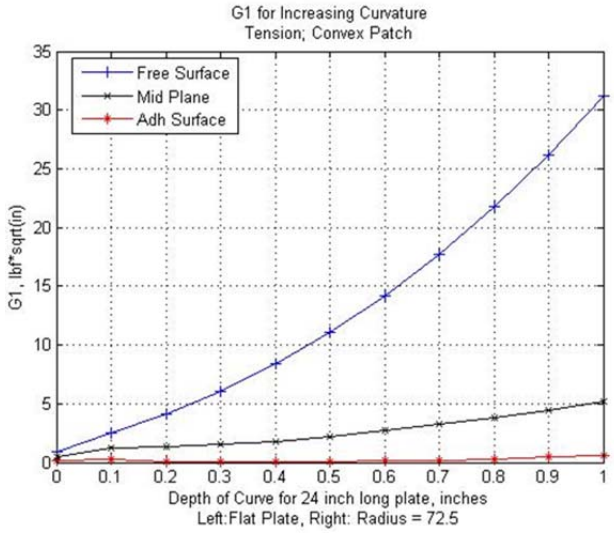

Figure 77. Change in radius, convex, tension

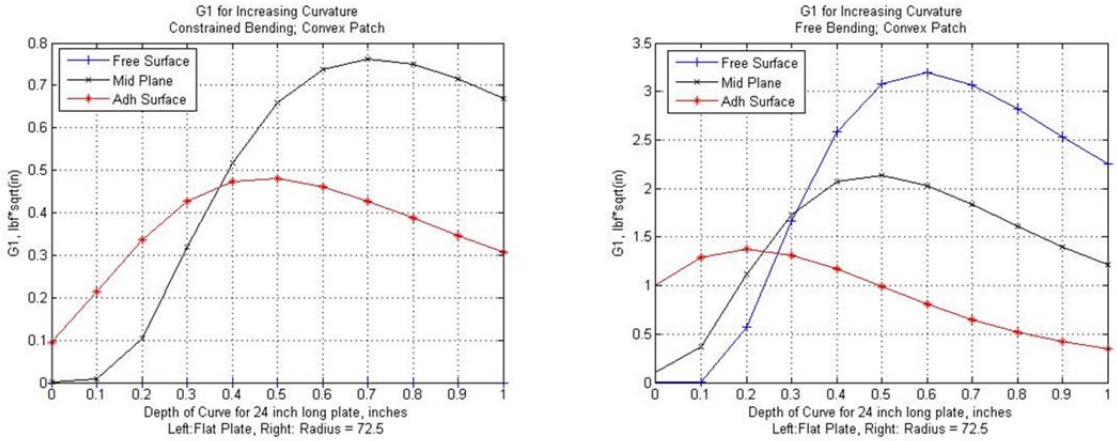

Figure 78. Change in radius, convex, Left = constrained bending, Right = free bending

2. Varied Dimensional Parameters

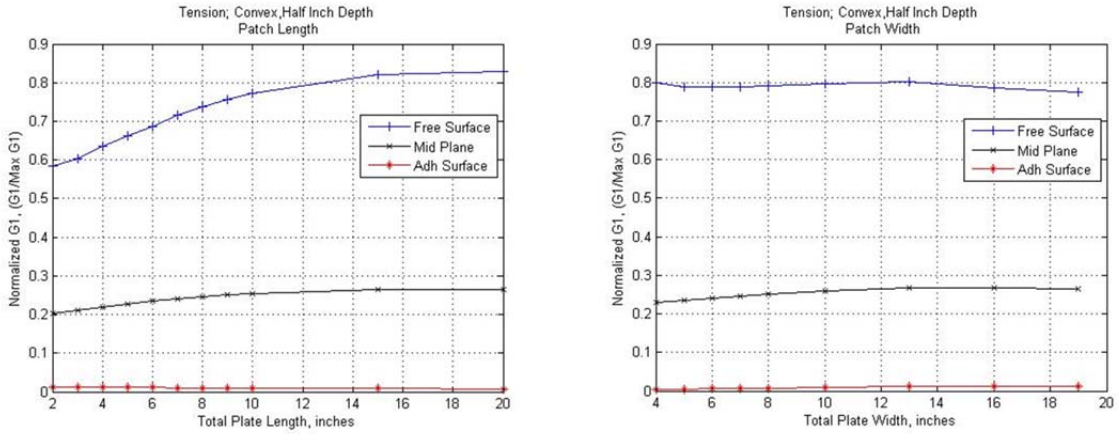

Figure 79. Convex, tension, 0.5-inch depth, Left = vary length, Right = vary width

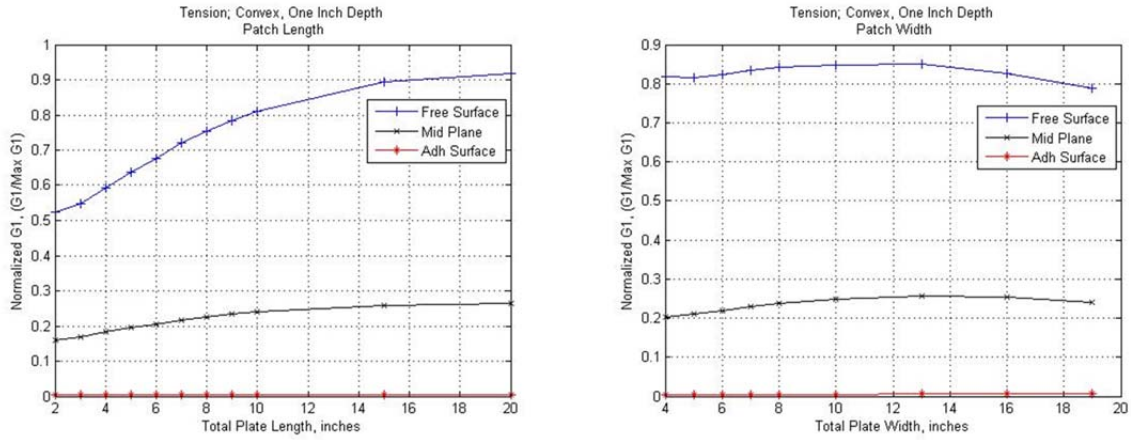

Figure 80. Convex, tension, 1-inch depth, Left = Vary length, Right = Vary Width

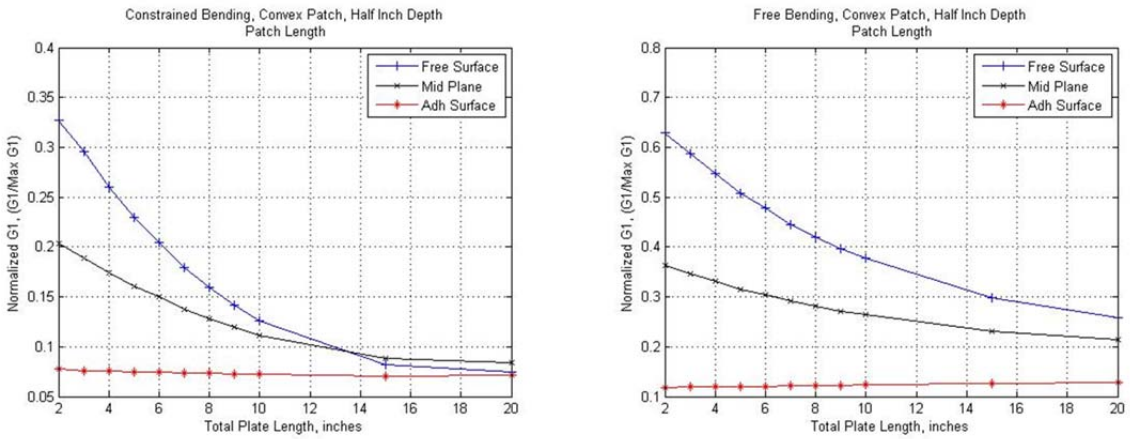

Figure 81. Convex, vary length, 0.5-inch depth, Left = constrained bending, Right = free bending

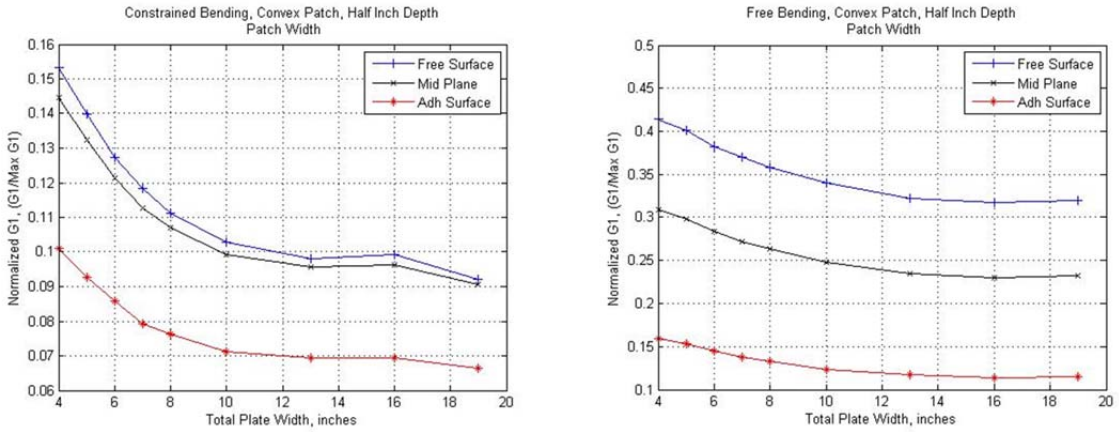

Figure 82. Convex, vary width, 0.5-inch depth, Left = constrained bending, Right = free bending

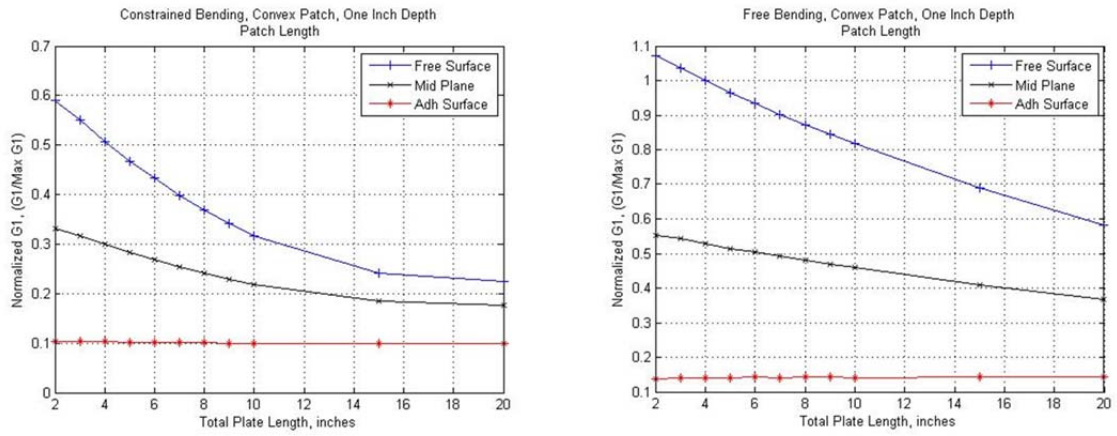

Figure 83. Convex, vary length, 1-inch depth, Left = constrained bending, Right = free bending

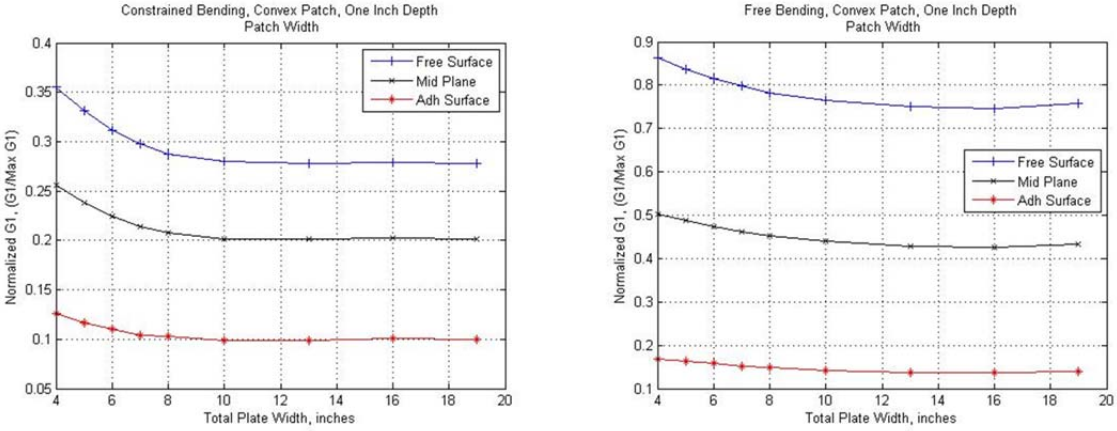

Figure 84. Convex, vary width, 0.5-inch depth, Left = constrained bending, Right = free bending

3. Constant Stiffness Ratio

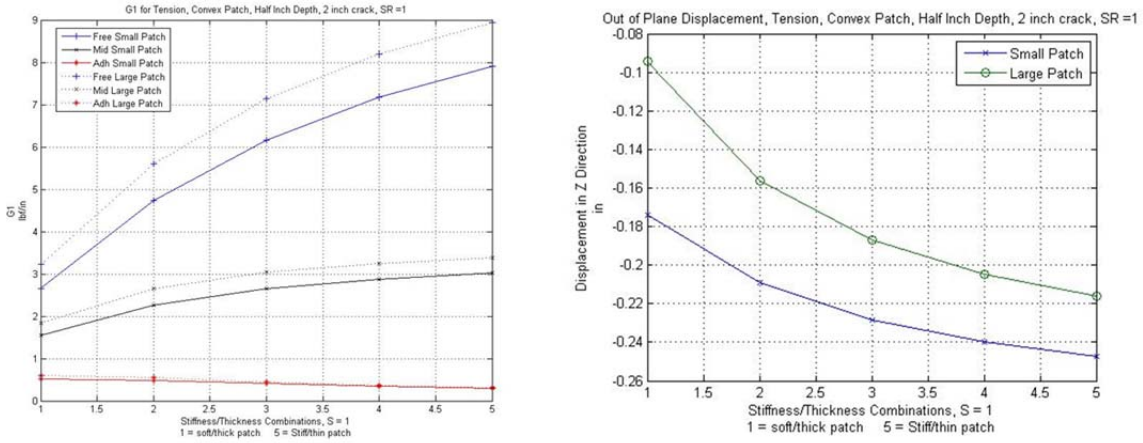

Figure 85. CS, tension, convex patch, 0.5-inch depth, 2-inch crack, Left = G1, Right = out of plane displacement

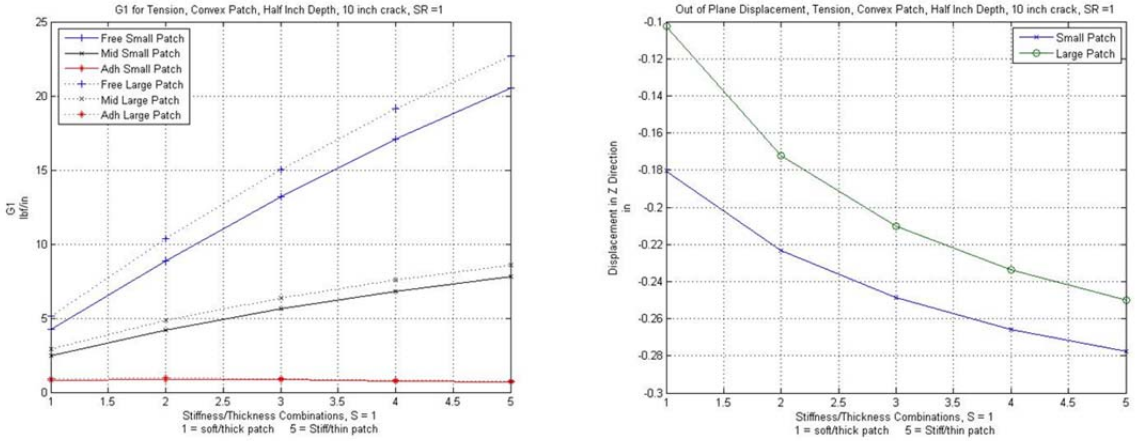

Figure 86. CS, tension, convex patch, 0.5-inch depth, 10-inch crack, Left = G1, Right = out of plane displacement

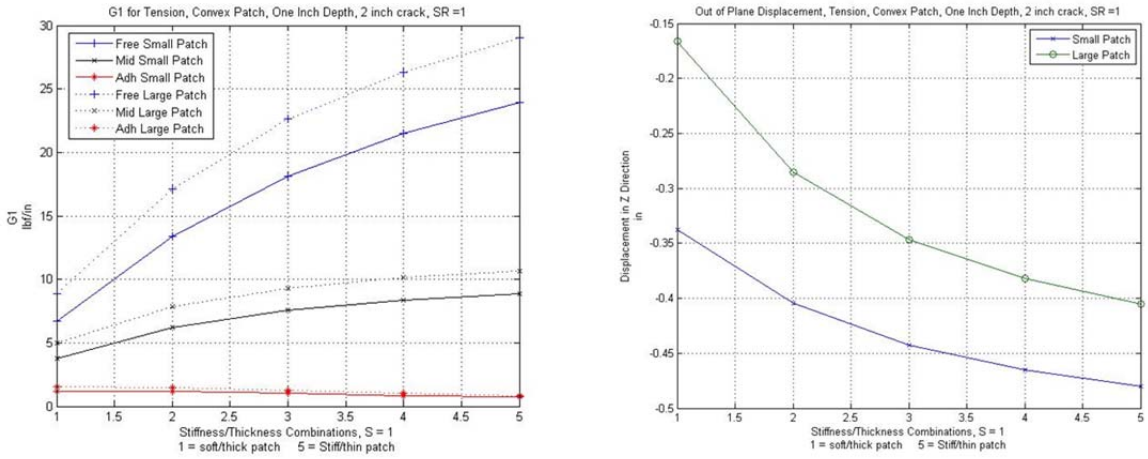

Figure 87. CS, tension, convex patch, 1-inch depth, 2-inch crack, Left = G1, Right = out of plane displacement

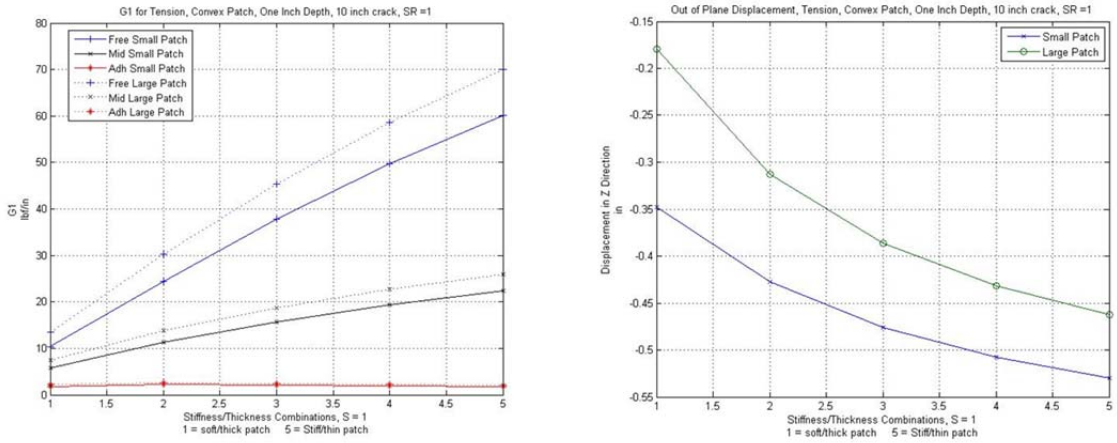

Figure 88. CS, tension, convex patch, 1-inch depth, 10-inch crack, Left = G1, Right = out of plane displacement

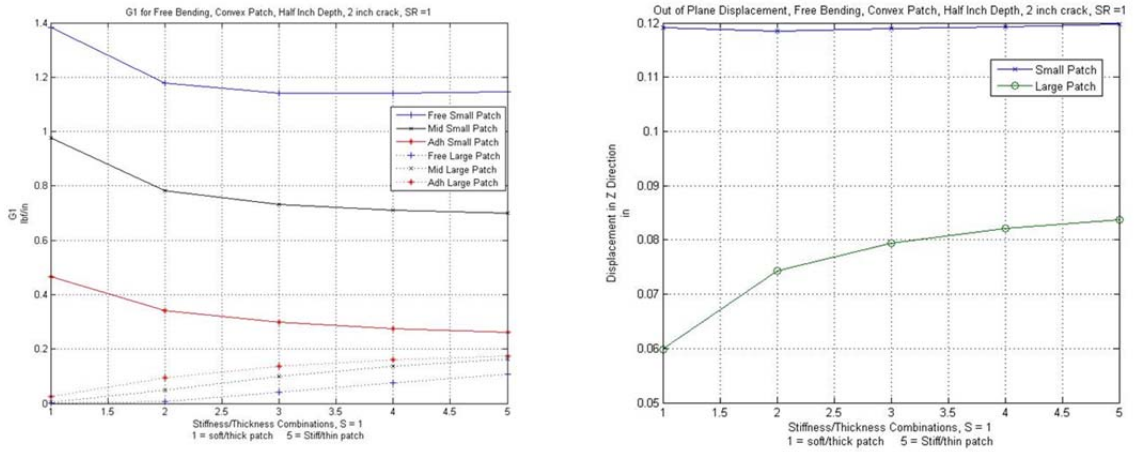

Figure 89. CS, free bending, convex patch, 0.5-inch depth, 2-inch crack, Left = G1, Right = out of plane displacement

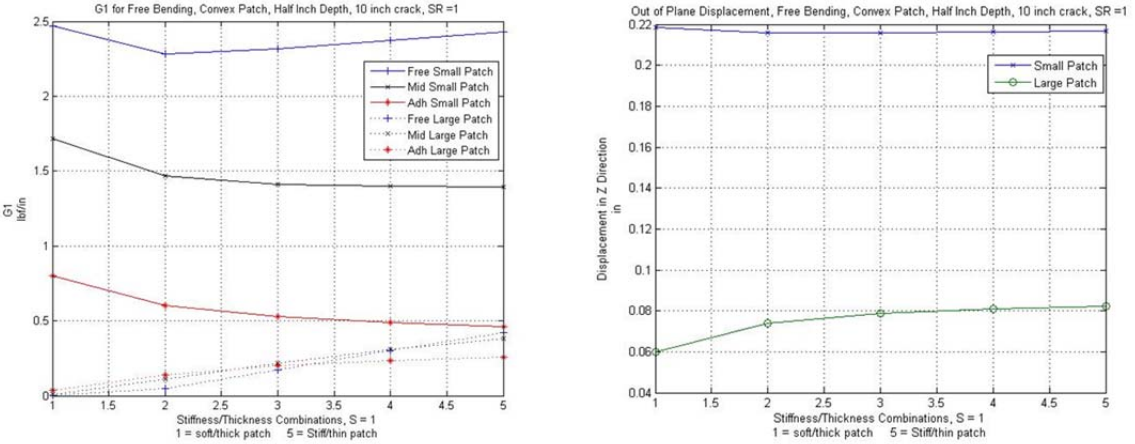

Figure 90. CS, free bending, convex patch, 0.5-inch depth, 10-inch crack, Left = G1, Right = out of plane displacement

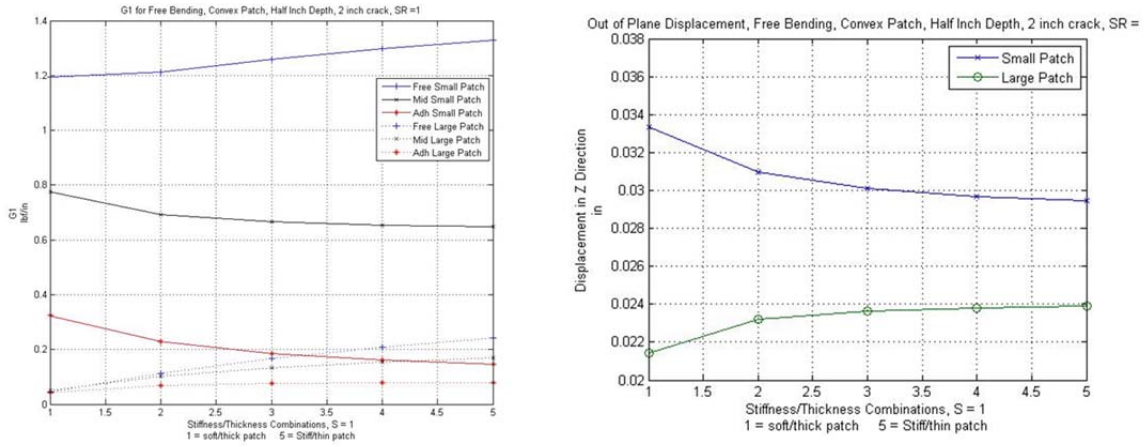

Figure 91. CS, free bending, convex patch, 0.5-inch depth, 2-inch crack, Left = G1, Right = out of plane displacement

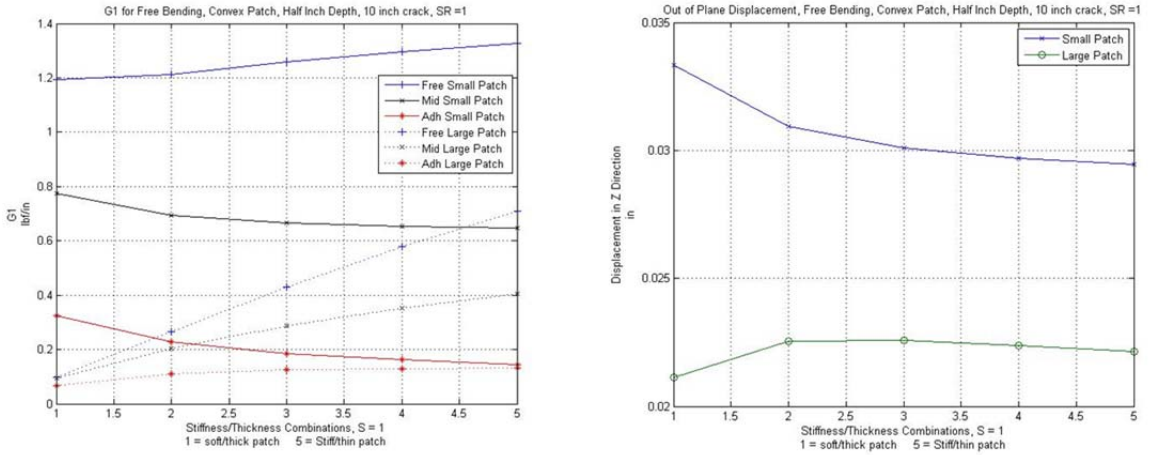

Figure 92. CS, free bending, convex patch, 0.5-inch depth, 10-inch crack, Left = G1, Right = out of plane displacement

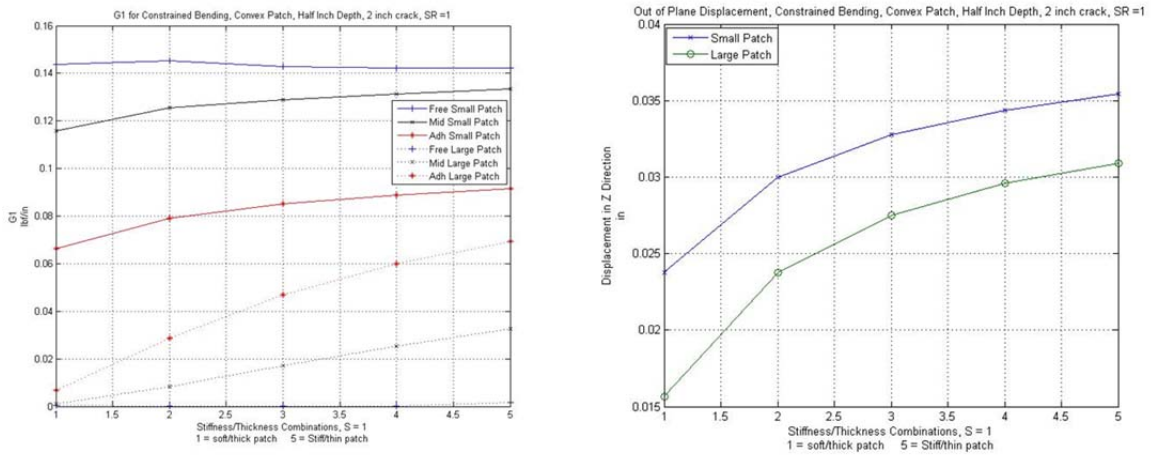

Figure 93. CS, constrained bending, convex patch, 0.5-inch depth, 2-inch crack, Left = G1, Right = out of plane displacement

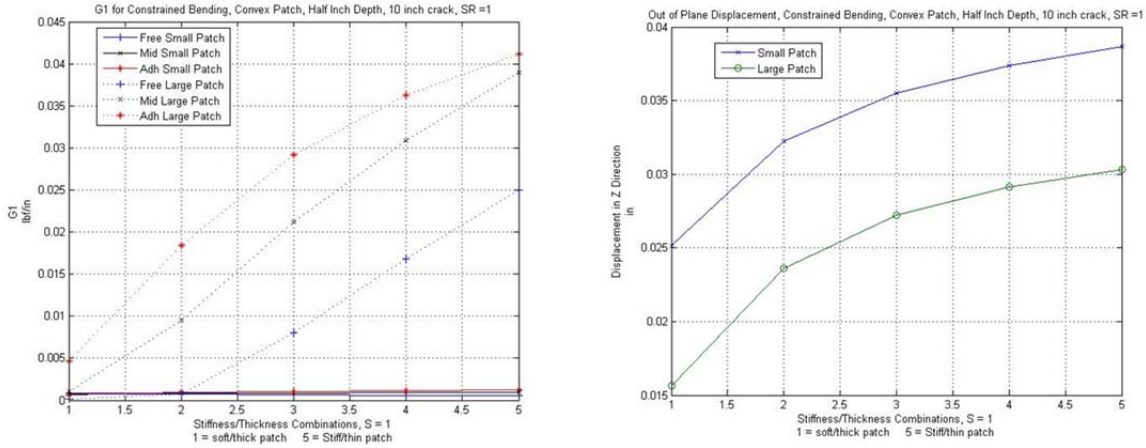

Figure 94. CS, constrained bending, convex patch, 0.5-inch depth, 10-inch crack, Left = G1, Right = out of plane displacement

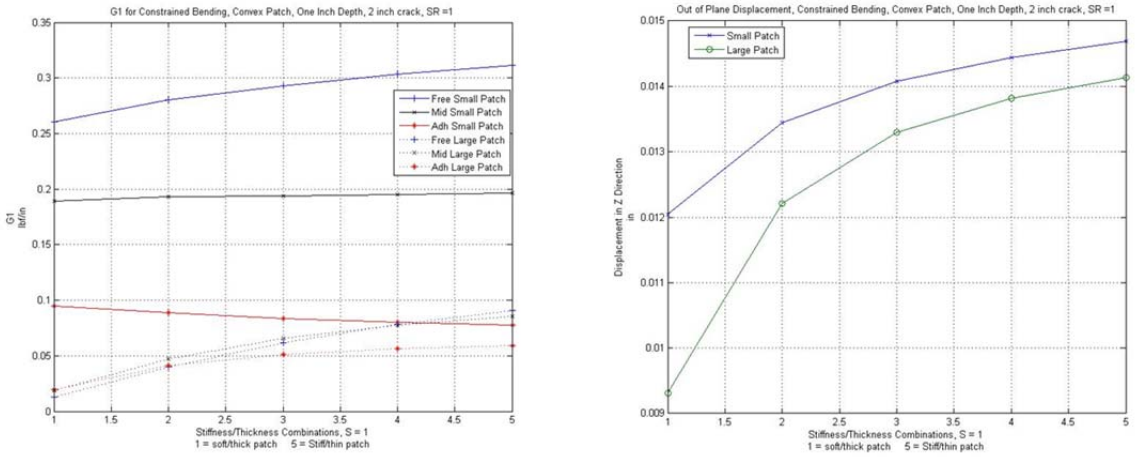

Figure 95. CS, constrained bending, convex patch, 1-inch depth, 2-inch crack, Left = G1, Right = out of plane displacement

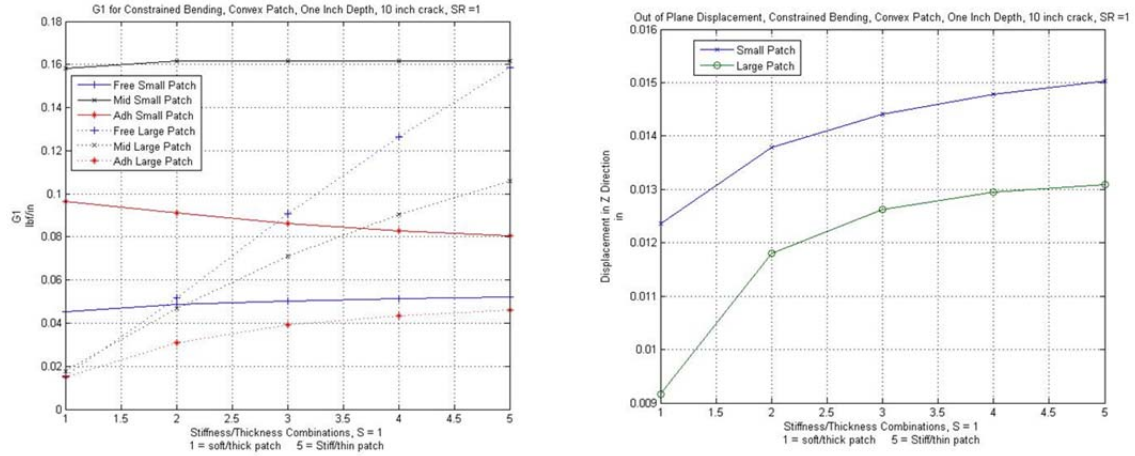

Figure 96. CS, constrained bending, convex patch, 1-inch depth, 10-inch crack, Left = G1, Right = out of plane displacement

THIS PAGE INTENTIONALLY LEFT BLANK

LIST OF REFERENCES

[1] NSWC Carderock Division, Code 65, "US Navy composite patch repair efforts for CG-46 class aluminum superstructures," presented at the Naval Postgraduate School, Monterey, CA, 2011.

[2] C. Duong and C. H. Wang, "Theory of bonded doublers and bonded joints," in *Composite Repair*, *Theory and Design*, Oxford, England: Elsevier, 2007, pp. 8–68.

[3] I. Grabovac and D. Whittaker, "Application of bonded composites in the repair of ships structures - A 15-year Service experience," *Composites: Part A,* vol. 40, no. 9, pp. 1381–1398, 2009.

[4] A. Echtermeyer, A. T. Echtermeyer, K. H. Leong, B. Melve, M. Robinson, and K. P. Fisher, "Repair of FPSO with bonded composite patches," in *Fourth International Conference On Composite Materials For Offshore Operations*, Houston, TX, 2005, pp. 1364–1380.

[5] I. Grabovac, "Bonded composite solution to ship reinforcement," *Composites Part A: Applied Science and Manufacturing,* vol. 34, no. 9, pp. 847–854, 2003.

[6] D. McGeorge, A. T. Echtermeyer, K. H. Leong, B. Melve, M. Robinson, and K. P. Fischer, "Repair of floating offshore units using bonded fibre composite materials," *Composites: Part A,* vol. 40, no. 9, pp. 1364–1380, 2009.

[7] M. Belhouari, B. B. Bouidjra, A. Megueni, and K. Kaddouri, "Comparison of double and single bonded repairs to symmetric composite structures: A numerical analysis," *Composite Structures,* vol. 65, no. 1, pp. 47–53, 2004.

[8] G.C. Tsai and S. B. Shen, "Fatigue analysis of cracked thick aluminum plate bonded with composite patches," *Composite Structures,* vol. 64, no. 1, pp. 79–90, 2004.

[9] K. Madani, S. Touzain, X. Feaugas, M. Benguediab, and M. Ratwani, "Numerical analysis for the determination of the stress intensity factors and crack opening displacements in plates repaired with single and double composite patches," *Computational Materials Science,* vol. 42, no. 3, pp. 385–393, 2008.

[10] C. H. Wang, L. R. F. Rose, and R. Callinan, "Analysis of out-of-plane bending in one-sided bonded repair," *International Journal of Solids and Structures,* vol. 35, no. 14, pp. 1653–1675, 1998.

[11] A. Kumar and S. Hakeem, "Optimum design of symmetric composite patch repair to centre cracked metallic sheet," *Composite Structures,* vol. 49, no. 3, pp. 285–292, 2000.

[12] A. Okafor, N. Singh, U. E. Enemouh, and S. V. Rao, "Design, analysis and performance of adhesively bonded composite patch repair of cracked aluminum aircraft panels," *Composite Structures,* vol. 71, no. 2, pp. 258–270, 2005.

[13] H. Hosseini-Toudeshky and B. Mohammadi, "Mixed-mode numerical and experimental fatigue crack growth analyses of thick aluminium panels repaired with composite patches," *Composite Structures,* vol. 91, no. 1, pp. 1–8, 2009.

[14] D. Ouinas, B. B. Bouiadjra, B. Achour, and N. Benderdouche, "Modelling of a cracked aluminium plate repaired with composite octagonal patch in mode I and mixed mode," *Materials and Design,* vol. 30, no. 3, pp. 590–595, 2009.

[15] C. Chue and T. J. Liu, "The effects of laminated composite patch with different stacking sequences on bonded repair," *Composites Engineering,* vol. 5, no. 2, pp. 223–230, 1995.

[16] H. Hosseini-Toudeshky, "Effects of composite patches on fatigue crack propagation of single-side repaired aluminum panels," *Composite Structures,* vol. 76, no. 2, pp. 243–251, 2006.

[17] H. Hosseini-Toudeshky, B. Mohammadi, G. Sadeghi, and H. R. Daghyani, "Numerical and experimental fatigue crack growth analysis in mode-I for repaired aluminum panels using composite material," *Composites: Part A,* vol. 38, no. 4, pp. 1141–1148, 2007.

[18] H. Hosseini-Toudeshky, G. Sadeghi, and H. Daghyani, "Experimental fatigue crack growth and crack-front shape analysis of asymmetric repaired aluminium panels with glass/epoxy composite patches," *Composite Structures,* vol. 71, no. 3-4, pp. 401–406, 2005.

[19] V. Sabelkin, S. Mall, M. A. Hansen, R. M. Vanawaker and M. Derris, "Investigation into cracked aluminum plate repaired with Bonded composite patch," *Composte Structures,* vol. 79, no. 1, pp. 55–66, 2007.

[20] C. Wang, L. R. F. Rose, R. Callinan and A. A. Baker, "Thermal Stresses in a Plate with a Circular Reinforcement," *International Journal of Solids and Structures,* vol. 37, no. 33, pp. 4577–4599, 2000.

[21] S. Naboulsi and S. Mall, "Thermal effects on adhesively bonded composite repair of cracked aluminum panels," *Theoretical and Applied Fracture Mechanics,* vol. 26, no. 1, pp. 1–12, 1997.

[22] C. Lilgedahl, M. Fitzpatrick and L. Edwards, "Residual stress in structures reinforced with adhesively bonded straps designed to retard fatigue crack growth," *Composite Structures,* vol. 86, no. 4, pp. 344–355, 2008.

[23] A. Deheeger, J. Mathias and M. Grediac, "A closed-form solution for the thermal stress distribution in rectangular metal/composite bonded joints," *International Journal of Adhesion and Adhesives,* vol. 29, no. 5, pp. 515–524, 2009.

[24] X. Sun and L. Tong, "Curvature effect on fracture toughness of cracked cylindrical shells bonded with patches," *AIAA Journal,* vol. 42, no. 12, pp. 2585–2591, 2004.

[25] X. Sun and S. Tong, "Fracture toughness analysis of inclined crack in cylindrical shell repaired with bondeds composite patch," *Composite Structures,* vol. 66, no. 3, pp. 639–645, 2004.

[26] L. Tong and X. Sun, “Adhesive elements for stress analysis of bonded patch to curved thin-walled structures,” *Computational Mechanics,* vol. 30, no. 2, pp. 143–154, 2003.

[27] L. Tong and X. Sun, “Nonlinear stress analysis for bonded patch to curved thin-walled structures,” *International Journal of Adhesion and Adhesives,* vol. 23, no. 5, pp. 349–364, 2003.

[28] *ANSYS Mechanical APDL Element Reference*, Canonsburg, PA: ANSYS Inc.

[29] C. Sun and H. Chin, “Analysis of Asymmetric Composite Laminates,” in *AIAA/ASME/ASCE/AHS 28th Structures, Structural Dynamics and Materials Conference*, Monterey, CA, 1987, pp. 714–718.

[30] *Theory Reference for Mechanical APDL and Mechanical Applications*, Canonsburg, PA: ANSYS Inc.

[31] R. Krueger, “The virtual crack closure technique: history, approach and Applications,” *NASA/CR-2002-211628,* pp. 1–59, April 2002.

[32] H. Hosseini-Toudeshky, M. Saber and B. Mohammadi, “Finite element crack propagation of adhesivly bonded repaired panels in general mixed-mode conditions,” *Finite Elements in Analysis and Design,* vol. 45, no. 45, pp. 94–103, 2009.

[33] H. Hosseini-Toudeshky, S. Bakhshandeh, B. Mohammadi and H. R. Dagyani, “Experimental investigation of fatigue crack growth of repaired thick aluminium panels in mixed-mode conditions,” *Composite Structures,* vol. 75, no. 1–4, pp. 437–443, 2006.

[34] ANSYS Technical Support (private communication), April 2012.

THIS PAGE INTENTIONALLY LEFT BLANK

INITIAL DISTRIBUTION LIST

1. Defense Technical Information Center
   Ft. Belvoir, Virginia

2. Dudley Knox Library
   Naval Postgraduate School
   Monterey, California

3. Prof. Young W. Kwon
   Naval Postgraduate School
   Monterey, California

4. Professor and Chairman Knox T. Millsaps
   Naval Postgraduate School
   Monterey, California

5. Jarema M. Didoscak
   Naval Postgraduate School
   Monterey, California

6. Erik A. Rasmussen
   Naval Surface Warfare Center Carderock Division
   West Bethesda, Maryland

7. Douglas C. Loup
   Naval Surface Warfare Center Carderock Division
   West Bethesda, Maryland

8. Daniel C. Hart
   Naval Surface Warfare Center Carderock Division
   West Bethesda, Maryland

9. Aaron S. McGee
   Naval Postgraduate School
   Monterey, California